Constructing Density Forecasts from Quantile Regressions: Multimodality in Macro-Financial Dynamics*

James Mitchell†, Aubrey Poon‡, and Dan Zhu§

January 21, 2024

Abstract

Quantile regression methods are increasingly used to forecast tail risks and uncertainties in macroeconomic outcomes. This paper reconsiders how to construct predictive densities from quantile regressions. We compare a popular two-step approach that fits a specific parametric density to the quantile forecasts with a nonparametric alternative that lets the "data speak." Simulation evidence and an application revisiting GDP growth uncertainties in the US demonstrate the flexibility of the nonparametric approach when constructing density forecasts from both frequentist and Bayesian quantile regressions. They identify its ability to unmask deviations from symmetrical and unimodal densities. The dominant macroeconomic narrative becomes one of the evolution, over the business cycle, of multimodalities rather than asymmetries in the predictive distribution of GDP growth when conditioned on financial conditions.

JEL Code: C53; E32; E37; E44

Keywords: Density Forecasts; Quantile Regressions; Financial Conditions

*Thanks to the Editor Barbara Rossi, two anonymous referees, Aaron Amburgey, Todd Clark, Gergely Ganics, Domenico Giannone, Gary Koop, Ed Knotek, Mike McCracken, Tatevik Sekhposyan, Benjamin Wong, Saeed Zaman, and participants at the ISF 2021, SNDE 2022, and an IIF MacroFor seminar for helpful comments. The views expressed herein are those of the authors and not necessarily those of the Federal Reserve Bank of Cleveland or the Federal Reserve System.

†Federal Reserve Bank of Cleveland; james.mitchell@clev.frb.org

‡University of Kent; A.Poon@kent.ac.uk

§Monash University; Dan.Zhu@monash.edu

1 Introduction

Recent research has used quantile regression (QR) methods both to produce density nowcasts and forecasts of macroeconomic and financial variables and to assess tail risks, emphasizing asymmetries in the distribution of (real) GDP growth when conditioned on financial conditions.[1] A commonly adopted approach in this literature, following Adrian, Boyarchenko, and Giannone (2019) [henceforth ABG], is to produce the density forecasts in two steps. As a first step, the QRs are estimated. This means that the underlying conditional density is defined only at the chosen quantiles (typically four quantiles are chosen). As a result, as a second step, the skewed-t density function of Azzalini and Capitanio (2003) is fitted to these quantile forecasts by minimizing the distance (the ℓ_2 norm) between the (empirical) regression quantiles and the (theoretical) density-implied quantiles. This second step both smooths the estimated quantile functions and provides a complete density forecast, albeit one whose form is now controlled by the class of skewed-t density assumed. This second step, therefore, contrasts with the nonparametric nature of the first-step quantile regressions. Policy institutions, such as the IMF, have also adopted this two-step approach to monitor international macroeconomic risks, such as growth-at-risk (GaR); see Prasad et al. (2019).

This paper reconsiders the use of QRs when interest rests with the production and subsequent evaluation of density forecasts, from which specific risk forecasts, such as GaR, can always be extracted. The attraction of producing density forecasts rather than specific point, quantile, or interval forecasts is that, given the forecast user's loss function, one can readily extract from the density forecast the features of specific interest to the user. Such a focus on the production of density forecasts is rare in the quantile regression literature (with the notable exceptions listed above), despite considerable attention having been paid to the production and evaluation of the quantile forecasts themselves (for example, see Komunjer (2013)).

Our paper proposes and then contrasts with the aforementioned two-step ABG method, which has become so established, a simple nonparametric (strictly "semi-parametric") approach to the production of density forecasts from QRs. Unlike ABG's, this approach does not superimpose a global density on specific quantile forecasts. Instead, the conditional quantile forecasts from the first-step QRs are mapped directly to a conditional density, assuming only local uniformity between the quantile forecasts. In an application to US GDP growth, we

[1] On the use of QR methods to produce density nowcasts and forecasts, see, e.g., Gaglianone and Lima (2012), Manzan and Zerom (2013), Gaglianone and Lima (2014), Manzan (2015), Korobilis (2017), Chen, Dolado, and Gonzalo (2021), Ferrara, Mogliani, and Sahuc (2022), and Mitchell, Poon, and Mazzi (2022). On the more specific but connected issue of the assessment of tail risks using QRs, see, e.g., Giglio, Kelly, and Pruitt (2016), Ghysels, Iania, and Striaukas (2018), Adrian, Boyarchenko, and Giannone (2019), Figueres and Jarocinski (2020), Reichlin, Ricco, and Hasenzagl (2020), Brownlees and Souza (2021), Carriero, Clark, and Marcellino (2022), and Carriero, Clark, and Marcellino (2023).

find that use of this nonparametric approach matches or slightly improves upon the accuracy of the ABG densities. It also supports the much-cited finding of ABG that the left-tail of the conditional density of GDP growth moves with the tightness of financial conditions. But the nonparametric approach delivers conditional forecast densities with very different features than those when, following ABG, a skewed-t density is assumed globally. In particular, linking to Adrian, Boyarchenko, and Giannone (2021), we find that the very same QRs used by ABG do, in fact, deliver multimodal GDP growth density forecasts. This is notably so at times of recession, when conditioning on a popular index of financial conditions. The evolution over the business cycle of multimodalities rather than asymmetries then becomes the dominant macroeconomic narrative of the conditional predictive distribution of GDP growth. But even though, especially when implemented as proposed in this paper, QRs can flexibly capture nonlinearities when forecasting, as a nonparametric (reduced-form) model they cannot so readily discriminate between alternative (more structural) explanations for the observed distributional properties of GDP growth. This would require stronger parametric assumptions.

This paper focuses on the construction of density forecasts from QRs, given their growing use in macroeconomics and finance since ABG. A large literature, of course, considers the production of density forecasts using other methods; see Aastveit et al. (2019) for a review. A literature has also grown up, in response to ABG, on the production of GaR and density forecasts using both parametric and nonparametric alternatives to QR; for example, see Caldara et al. (2021), Plagborg-Moller et al. (2020), Adrian, Boyarchenko, and Giannone (2021), Carriero, Clark, and Marcellino (2023), and Delle Monache, De Polis, and Petrella (2023). By contrast, we deliberately stick to the QR models of ABG. In so doing, we emphasize the empirical importance of moving beyond their skewed-t parametric assumption when fitting the density to these quantile forecasts.

The remainder of this paper is structured as follows. Section 2 considers the construction of density forecasts from quantile regressions, estimated via frequentist or Bayesian methods. It contrasts parametric and nonparametric methods for the production of the density forecast. Section 3 presents Monte Carlo evidence on the relative efficacy of the parametric and nonparametric approaches at fitting densities to distributions of various underlying shapes. Section 4 revisits the GaR application of ABG and contrasts empirical results using the parametric and nonparametric approaches. Section 5 concludes. An online appendix contains supplementary material.

2 Density forecasts from quantile regressions

Consider the QR relating the τ-th quantile of y_{t+h}, the variable of interest (GDP growth in our application), to x_t, a $d-$dimensional vector of conditioning variables including an intercept:

$$Q_\tau(y_{t+h}|x_t) = x_t'\beta_\tau, \tau \sim U(0,1), \tag{1}$$

with $t = 1, ..., T$ and where h is the forecast horizon and $U(.)$ is the uniform density. Note that, following ABG, we focus on QR models with time-invariant parameters.[2]

The QR slope, β_τ, is chosen to minimize the weighted absolute sum of errors:

$$\hat{\beta}_\tau = \arg\min_{\beta_\tau} \sum_{t=1}^{T-h} (\tau \mathbf{1}_{(y_{t+h} \geq x_t'\beta_\tau)} |y_{t+h} - x_t'\beta_\tau| + (1-\tau)\mathbf{1}_{(y_{t+h} \leq x_t'\beta_\tau)} |y_{t+h} - x_t'\beta_\tau|), \ \tau \in (0,1), \tag{2}$$

where $\mathbf{1}(.)$ denotes an indicator function. A perceived attraction of QR is that the informational importance of x_t for y_{t+h} can vary by quantile and thereby accommodate situations where conditioning variables have, for example, more or less informational content in the tails of the density.

The quantile forecasts from (2), conditional on x_t, are:

$$\hat{Q}_\tau(y_{t+h}|x_t) = x_t'\hat{\beta}_\tau. \tag{3}$$

Bayesian estimation of QRs has also gained attention recently. Koenker and Machado (1999) established that likelihood-based inference using independently distributed asymmetric Laplace densities (ALD) is directly related to (2). Yu and Moyeed (2001) show how exact Bayesian inference using Markov chain Monte Carlo (MCMC) methods can proceed by forming the likelihood function using the ALD; they emphasize the utility of the ALD, irrespective of the original distribution of the data. And Kozumi and Kobayashi (2011) propose a mixture representation of the ALD that renders the model conditionally Gaussian, facilitating estimation using more efficient MCMC methods. Unlike classical estimation methods, Bayesian methods naturally accommodate parameter uncertainty when forecasting. While a bootstrap-based approach, for example, could in principle be used to construct quantile forecasts that acknowledge parameter estimation error from QRs estimated via classical methods, in practice this is not undertaken, certainly in the ABG-inspired GaR literature.

[2]Recent research in macroeconomics has moved on to consider QR models with time-varying parameters (e.g., see Korobilis et al. (2021)). The same issues, as discussed in this paper, arise when considering how to construct density forecasts from these QR models.

Quantile forecasts can be constructed from the Bayesian QR, as per (3), by sampling from the posterior parameter distribution for β_τ. For the r-th ($r = 1, ..., R$) MCMC draw, $\hat{\beta}_\tau^r$, these quantile forecasts are given as:

$$\hat{Q}_\tau(y_{t+h}|x_t)^r = x_t'\hat{\beta}_\tau^r. \tag{4}$$

In empirical applications, quantile regressions are estimated at a finite number of τ, i.e., $[\tau_1, ..., \tau_k]$, where $0 < \tau_1 < \tau_2 < .... < \tau_k < 1$. ABG, in fact, consider just $k = 4$. This means that the underlying conditional density is defined only at these k quantiles. To estimate the full conditional $h-$step-ahead predictive density, $\hat{f}(y_{t+h}|x_t)$, we therefore need to establish a mapping from the k quantile forecasts, as in (3) or (4):

$$\left\{\hat{Q}_{\tau_1}(y_{t+h}|x_t), ..., \hat{Q}_{\tau_k}(y_{t+h}|x_t)\right\} \rightarrow \hat{f}(y_{t+h}|x_t), \forall [x_t', y_{t+h}]' \in \mathbb{R}^{dim(x)+1}, \tag{5}$$

where, for notational ease, we denote these quantile forecasts $\hat{Q}_{\tau_j}(y_{t+h}|x_t) = x_t'\hat{\beta_{\tau_j}}$; that is, we suppress dependence on the MCMC draw for the case when the QR is estimated via Bayesian methods.

Below we set out two ways of establishing this mapping. We start with the parametric approach of ABG. As discussed in the introduction, this approach is used widely in macroeconomics, despite the contradiction with the nonparametric flavor of the first-step QRs.

2.1 ABG's parametric quantile-matching approach

To estimate the full continuous conditional density forecast of y_{t+h}, from the k quantile forecasts, ABG, in effect, combine them by fitting the skewed-t density function of Azzalini and Capitanio (2003) to the quantile forecasts, (3). They minimize the distance (the ℓ_2 norm) between the (empirical) regression quantiles and the (theoretical) distribution-implied quantiles:

$$\underset{\mu,\sigma,\alpha,\upsilon}{arg\ min} \sum_\tau \left(\hat{Q}_\tau(y_{t+h}|x_t) - \hat{F}^{-1}(\tau; \mu, \sigma, \alpha, \upsilon)\right)^2, \tag{6}$$

where F is the CDF of the skewed-t PDF, f, given as:

$$f(y; \mu, \sigma, \alpha, \upsilon) = \frac{2}{\sigma} t\left(\frac{y-\mu}{\sigma}; \upsilon\right) T\left(\alpha \frac{y-\mu}{\sigma} \sqrt{\frac{\upsilon+1}{\upsilon + \left(\frac{y-\mu}{\sigma}\right)^2}}; \upsilon+1\right), \tag{7}$$

where t and $T(.)$ respectively denote the PDF and CDF of the Student t-distribution, where μ is a location parameter, σ is the scale, υ is the fatness, and α is the shape. When $\alpha = 0$, the skewed-t reduces to the Student t. When, in addition, $\upsilon = \infty$, (7) reduces to a Gaussian

distribution, with mean μ and standard deviation σ.

ABG focus on the exactly identified case of matching the 0.05, 0.25, 0.75, and 0.95 quantiles. But, in principle, as ABG discuss in a footnote but do not explore empirically, more quantiles could be used, allowing the four parameters of (7) to be over-identified. Since the choice of these $k = 4$ quantiles is somewhat arbitrary and may affect the shape of the fitted distribution, below we also consider fitting the skewed-t distribution to more quantiles.

While ABG used (6) on quantile forecasts, (3), produced from a frequentist QR, others have fitted the skewed-t distribution to forecasts produced from a Bayesian QR. Ferrara, Mogliani, and Sahuc (2022), for example, use (6) on the mean (across $r = 1, ..., R$ MCMC draws) quantile forecasts, (4).

2.2 Constructing the density forecast nonparametrically

Rather than assume a parametric function for $\hat{f}(y_{t+h}|x_t)$, following Parzen (1979) and Koenker (2005), one can back out the conditional distribution directly from the conditional quantile function via the integral transforms:

$$\hat{F}(y_{t+h}|x_t) = \int_0^1 \mathbf{1}\{x_t'\hat{\beta}_\tau \leq y_{t+h}\}d\tau. \tag{8}$$

By considering all $\tau \in (0, 1)$, one can approximate the true conditional quantile function arbitrarily well, when the true density is a smooth conditional density (Koenker (2005), p. 53).

In practice, we follow Koenker and Zhao (1996) and adopt a simple simulation-based approach, instead of relying on numerical integration. Random draws are taken from the h-step-ahead forecast distribution given by:

$$\hat{y}_{t+h} = \hat{Q}_U(y_{t+h}|x_t), \tag{9}$$

where U is a uniformly distributed random variable on $[0, 1]$ as in Koenker and Zhao (1996). Repeating across many random draws approximates $\hat{F}(y_{t+h}|x_t)$.

To operationalize, with a finite k, we smooth/interpolate across adjacent quantile forecasts by taking a first-order Taylor expansion of the CDF, (8), for a value y_{t+h} between the j-th and $(j + 1)$-th conditional quantiles for $j = 1, ..., k - 1$:

$$\hat{F}_k(y_{t+h}|x_t) = \tau_j + \frac{\tau_{j+1} - \tau_j}{x_t'\hat{\beta}_{\tau_{j+1}} - x_t'\hat{\beta}_{\tau_j}}(y_{t+h} - x_t'\hat{\beta}_{\tau_j}) \tag{10}$$

$$= \tau_j + F'(y^*_{t+h,j}|x_t)(y_{t+h} - x_t'\hat{\beta}_{\tau_j}), \tag{11}$$

for $y^*_{t+h,j} \in \left(x_t'\hat{\beta}_{\tau_j}, y_{t+h}\right) \subset \left(x_t'\hat{\beta}_{\tau_j}, x_t'\hat{\beta}_{\tau_{j+1}}\right)$. Assuming that the interval between adjacent quantiles is relatively small, the implied distribution function is approximately linear within the interval.

Figure 1 provides an illustration, plotting the approximate CDF in yellow and the true CDF in blue. This illustration intuitively points to higher values of k delivering better approximations. That is, the marginal benefits of the first-order approximation decline as k increases, an issue we explore below in both the simulations and the application. Unlike ABG's, this approach does not superimpose a global (parametric, such as a skewed-t) distribution on specific quantile forecasts. Instead, it assumes local uniformity between the k quantile forecasts. Hence, it is best seen as a "semi-parametric" method, although for convenience we continue to refer to the method as nonparametric.

Algorithm 1 summarizes the mechanics of how the density forecast is formed nonparametrically from the QRs. Whether the QRs are estimated by frequentist or Bayesian methods, the empirical density forecast is constructed from the NR-dimensional vector: $\left[\boldsymbol{y}'_{t+h,1}, \boldsymbol{y}'_{t+h,2}, ..., \boldsymbol{y}'_{t+h,k}, \boldsymbol{y}'_{t+h,k+1}\right]'$, where N is the number of draws taken from the conditional density forecast (via Algorithm 1) and R ($R = 1$ for frequentist QR) is the number of MCMC draws used if the QR is estimated via Bayesian methods. This vector can be used directly by the macroeconomist or a kernel could be fitted.[3]

We note four features of Algorithm 1:

1. Since:

$$Prob(F^{-1}(\tau_j|x_t) \leq y_{t+h} < F^{-1}(\tau_{j+1}|x_t)) = \tau_{j+1} - \tau_j, \tag{12}$$

   to take a sample of length N from the conditional distribution $F(\cdot|X = x_t)$ requires $(\tau_{j+1} - \tau_j)N$ samples to be taken between:

$$\left(x_t'\hat{\beta}_{\tau_j}, x_t'\hat{\beta}_{\tau_{j+1}}\right). \tag{13}$$

2. The quantile forecasts are re-arranged as necessary (following Chernozhukov, Fernández-

[3]See Krüger et al. (2021) for a discussion of the pros and cons of alternative methods for estimating the distribution from the underlying simulation output. Their analysis demonstrates that the empirical CDF-based approximation works well in many contexts.

Algorithm 1 A local-linear algorithm to construct density forecasts from quantile regressions

- Estimate the QR at τ_j $(j = 1, ..., k)$. For Bayesian QR, repeat the steps below for each MCMC draw, $\hat{\beta}^r_{\tau_j}$, $r = 1, ..., R$.

- Denote the QR estimates, $\hat{\beta}_{\tau_j}$, where for Bayesian estimation $\hat{\beta}_{\tau_j} = \hat{\beta}^r_{\tau_j}$. Define:

$$Q_t = \left[(x_t{}'\hat{\beta}_{\tau_1}), (x_t'\hat{\beta}_{\tau_2}), ..., (x_t'\hat{\beta}_{\tau_k}) \right]' .$$

- Rearrange the elements of the $k \times 1$ vector Q_t from smallest to largest, in case they are not monotonic.

- for $j = 2 : k$

  - Construct a $(\tau_j - \tau_{j-1})N$ vector of forecasts, $\boldsymbol{y}_{t+h,j}$, by taking uniform draws between $[\tilde{Q}_{t,j-1}, \tilde{Q}_{t,j}]$:

$$\boldsymbol{y}_{t+h,j} = \tilde{Q}_{t,j-1}\mathbf{1}_{(\tau_j - \tau_{j-1})N} + (\tilde{Q}_{t,j} - \tilde{Q}_{t,j-1})U_j$$

    where N is the total number of draws from the density forecast, $\tilde{Q}_{t,j}$ denotes the jth element of Q_t, $\mathbf{1}_{(\tau_j - \tau_{j-1})N}$ is a $(\tau_j - \tau_{j-1})N$ row vector of ones, and U_j is a $(\tau_j - \tau_{j-1})N$ row vector, with each element drawn from a standard uniform distribution similar to (9).

- end

- Given $\hat{\beta}_{\tau_1}$ and $\hat{\beta}_{\tau_2}$, fit a Gaussian (or some other) distribution to the left tail and then take $N\tau_1$ random draws from this fitted density when $F(y_{t+h}|x_t) < \tau_1$, to obtain the $N\tau_1$ row vector, $\boldsymbol{y}_{t+h,1}$.

- Given $\hat{\beta}_{\tau_{k-1}}$ and $\hat{\beta}_{\tau_k}$, fit a Gaussian (or some other) distribution to the right tail and then take $N(1 - \tau_k)$ random draws from this fitted density when $F(y_{t+h}|x_t) > \tau_k$, to obtain the $N(1 - \tau_k)$ row vector, $\boldsymbol{y}_{t+h,k+1}$.

Create a N-dimensional vector of forecasts: $\left[\boldsymbol{y}'_{t+h,1}, \boldsymbol{y}'_{t+h,2}, ..., \boldsymbol{y}'_{t+h,k}, \boldsymbol{y}'_{t+h,k+1}\right]'$. For Bayesian QR, also stack across r to create a NR-dimensional vector of forecasts.

Val, and Galichon (2010)) to avoid quantile crossing.

(a) The density is fitted beyond the outer or "extreme" quantiles, defined by τ_1 and τ_k, by assuming that a specific CDF applies in the tails.[4] The researcher is free to assume that any parametric CDF of their choosing applies in the tails. We focus on the case:

$$\Phi(x_t'\beta_{\tau_1}, \mu_1, \sigma_1) = \tau_1, \Phi(x_t'\beta_{\tau_2}, \mu_1, \sigma_1) = \tau_2 \tag{14}$$

$$\Phi(x_t'\beta_{\tau_{k-1}}, \mu_2, \sigma_2) = \tau_{k-1}, \Phi(x_t'\beta_{\tau_k}, \mu_2, \sigma_2) = \tau_k, \tag{15}$$

where Φ is the Gaussian CDF, and we solve for $[\mu_1, \sigma_1]$ to satisfy (14) and $[\mu_2, \sigma_2]$ to satisfy (15). In our application, results are robust to this choice. This is understood by noting that this Gaussianity assumption affects only the behavior of the extreme tails of the density forecasts constructed via Algorithm 1.[5] In addition to the question of how to fit the density beyond the outer quantiles defined by τ_1 and τ_k, it is well known that estimation of extreme quantiles with small samples can lead to coefficient bias; see Chernozhukov (2005). In small sample applications, the researcher may therefore prefer to estimate the extreme quantiles using extremal methods or Bayesian QR with shrinkage rather than frequentist QR. Alternatively, rather than estimate the extreme quantiles directly, increased power in small samples could be gained by simultaneously estimating the QR across multiple τ including the extreme quantiles. In the online appendix (Section A.2), to illustrate how our algorithm can be operationalized in such situations, we present results where we adapt the composite QR method (Zou and Yuan, 2008), and when $k = 99$ ($\tau \in [0.01, 0.02, ..., 0.99]$) we estimate a pooled QR in the extreme left tail as follows:

$$\arg \min_{b_1,..b_K,\beta} \sum_{j=1}^{K} \left\{ \sum_{t=1}^{T} \rho_{\tau_j} \left(y_{t+h} - b_j - x_t'\beta \right) \right\}$$

where b_j denotes the quantile-specific intercept and β denote the common (across

[4] In our simulations and the application, we define "extreme" as those quantiles either beyond 0.05 and 0.95 or beyond 0.01 and 0.99.

[5] In Section A.2 of the online appendix we present results when, instead of the Gaussian distribution, we assume that the generalized extreme value (EV) distribution of type 1 applies in the tails. The EV density is commonly used when undertaking inference of extremal QRs; see Chernozhukov (2005). When repeating the main empirical exercises in the main paper using the EV rather than the Gaussian distribution in the tails, we find that the densities both look and forecast similarly. We also experimented with the student-t CDF in the tails, to acknowledge that fatness in the extreme tails may be helpful. Again we find that our empirical results are little different, although the t density does introduce some extra "wiggles" into the extreme tails. Ultimately, the choice of what density to assume for the outer quantiles is an empirical question to be decided on an application-by-application basis.

quantiles) slope coefficients for $\tau_1, ...\tau_K \leq 0.05$, and similarly for the right tail quantiles ≥ 0.95. In this application, use of composite QR methods does not improve forecast accuracy. Note that for the pooled QR we exclude the intercept from x_t.

3. Algorithm 1 consistently estimates the true conditional distribution $F(y_{t+h}|x_t)$ as $T, k \to \infty$. This is understood by noting that there are two convergence aspects to consider in Algorithm 1: (a) statistical convergence, $T \to \infty$, and (b) convergence of the approximate distribution to the true distribution as the number of quantile levels, $k \to \infty$:

   (a) The consistency of the QR estimates $\hat{\beta_{\tau_j}}$ as $T \to \infty$ (see Chernozhukov, Fernández-Val, and Galichon (2010) and Koenker (2005)), at the chosen quantile levels, j, implies that the approximate distribution $\hat{F}_k \to F_k$. That is, referring again to Figure 1, the approximate distribution converges to the piecewise-linear function (the yellow line) approximating the true CDF (the blue line) at the chosen quantile. For $\tau \in \{\tau_1, ..., \tau_k\}$:

   $$F_k(x_t'\beta_\tau|x_t) = F(x_t'\beta_\tau|x_t), \tag{16}$$

   i.e., the vertex of the function equals the true density at the finite sequence of quantile levels (and the blue and yellow lines equal each other).

   (b) As $k \to \infty$, the piecewise-linear CDF (the yellow line in Figure 1) will converge to the true distribution (the blue line in Figure 1) between these quantile levels. This is seen as follows. Given a smoothness assumption for the true density, by Taylor's theorem, rewrite the true distribution as:

   $$F(y_{t+h}|x_t) = \tau_j + f(y^*_{t+h,1}|x_t)(y_{t+h} - x_t'\beta_{\tau_j}), \tag{17}$$

   for any $y_{t+h} \in \left(x_t'\beta_{\tau_j}, x_t'\beta_{\tau_{j+1}}\right)$ and some $y^*_{t+h,1} \in \left(x_t'\beta_{\tau_j}, y_{t+h}\right)$. Then, by the mean value theorem, the approximate k quantile level distribution is:

   $$F_k(y_{t+h}|x_t) = \tau_j + \frac{\tau_{j+1} - \tau_j}{x_t'\beta_{\tau_{j+1}} - x_t'\beta_{\tau_j}}(y_{t+h} - x_t'\beta_{\tau_j}) \tag{18}$$

   $$= \tau_j + f(y^*_{t+h,2}|x_t)(y_{t+h} - x_t'\beta_{\tau_j}), \tag{19}$$

   for $y^*_{t+h,2} \in \left(x_t'\beta_{\tau_j}, x_t'\beta_{\tau_{j+1}}\right)$ and $j = 1, ..., k-1$. Comparing (17) and (19), the only

Figure 1: Illustrative comparison of the true CDF against Algorithm 1 (F_k) and the CDF assuming uniform (equal) weights between adjacent quantiles: As $k \to \infty$, $\tau_{j+1} - \tau_j \to 0$

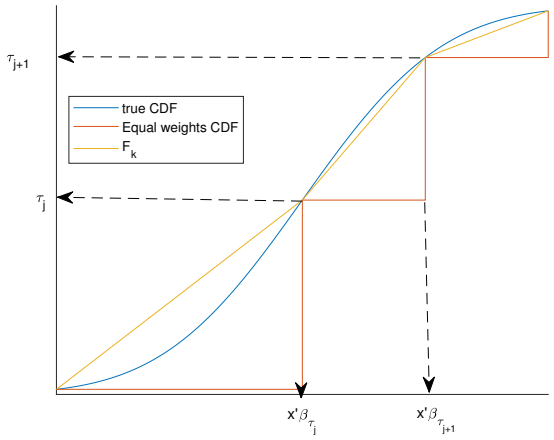

difference is between $y^*_{t+h,1}$ and $y^*_{t+h,2}$. Yet, note that:

$$x_t'\beta_{\tau_j} \leq y^*_{t+h,2} \leq x_t'\beta_{\tau_{j+1}} \tag{20}$$

$$x_t'\beta_{\tau_j} \leq y^*_{t+h,1} \leq y_{t+h} \leq x_t'\beta_{\tau_{j+1}}. \tag{21}$$

Further assume that the conditional quantiles are linear in the regressors, uniformly across all τ. Then, we can let $k \to \infty$. As $k \to \infty$, $\tau_{j+1} - \tau_j \to 0$, and the intervals in (20) and (21) converge by the sandwich theorem such that:

$$y^*_{t+h,1} = y^*_{t+h,2}.$$

Hence:

$$\lim_{k\to\infty} F_k(y_{t+h}|x_t) = F(y_{t+h}|x_t).$$

In the simulations and empirical application below, we consider how to choose k. We suggest, in effect, to choose k empirically to maximize forecasting performance. In general, we find that intermediate values of k (such as $k = 19$) tend to work best. These balance the need for a value large enough to accurately trace out the shape of the underlying distribution, with the risk, especially in smaller samples, of introducing noise by estimating QRs in the tails of the distribution with too few observations.

Algorithm 1, where the proposed distribution is:

$$\hat{F}_k(y_{t+h}|x_t) = \tau_j + \frac{\tau_{j+1} - \tau_j}{x_t'\hat{\beta}_{\tau_{j+1}} - x_t'\hat{\beta}_{\tau_j}}(y_{t+h} - x_t'\hat{\beta}_{\tau_j}), \tag{22}$$

when $y_{t+h} \in \left(x_t'\hat{\beta}_{\tau_j}, x_t'\hat{\beta}_{\tau_{j+1}}\right)$, can be contrasted with an alternative of using equal weights between adjacent quantiles:

$$\hat{F}_{EW}(y_{t+h}|x_t) = \begin{cases} \tau_j & y_{t+h} \in (x_t'\hat{\beta}_{\tau_j}, x_t'\hat{\beta}_{\tau_{j+1}}) \\ 0 & y_{t+h} < x_t'\hat{\beta}_{\tau_1} \\ 1 & y_{t+h} \geq x_t'\hat{\beta}_{\tau_k} \end{cases}, \tag{23}$$

which amounts to a zero-order approximation of the CDF between quantiles j and *j+1*. We emphasize that this is, in effect, the approach used by Korobilis (2017) to produce density forecasts from Bayesian QRs. This approach involves collecting together the $r = 1, ..., R$ MCMC draws of the quantile forecast $\widehat{Q}_{y_{T+h}}(\tau|x_t)^r$ across $\tau \in [0.05, 0.10, ..., 0.90, 0.95]$ and then constructing the full posterior density forecast from this stacked vector - using a kernel to smooth.

Figure 1 also illustrates how equal weights differ from Algorithm 1. It shows how equal weights intuitively provide a worse approximation to the true CDF, although, as with Algorithm 1, the quality of its approximation will improve as k increases. Indeed, as $k \to \infty$ the difference between Algorithm 1 and equal weights disappears; of course in practice, for finite T, the econometrician can only estimate a finite number of QRs. Note that, given the estimated quantile levels, the straight lines that Algorithm 1 imposes between adjacent quantiles provide a piecewise-linear approximation to the CDF. Unlike the piecewise-constant function implied by equal weights, the piecewise-linear approximation benefits from smoothness in the estimated CDF. Statistics such as the conditional mean can be obtained via numerical integration of:

$$\int x_t \hat{f}_k(y_{t+h}|x_t)dx_t, \tag{24}$$

where:

$$\hat{f}_k(y_{t+h}|x_t) = \begin{cases} \phi(y_{t+h}|\hat{\mu_1}, \hat{\sigma}_1) & y_{t+h} \leq x_t'\hat{\beta}_{\tau_1} \\ \frac{\tau_{j+1} - \tau_j}{x_t'\hat{\beta}_{\tau_{j+1}} - x_t'\hat{\beta}_{\tau_j}} & x_t'\hat{\beta}_{\tau_j} < y_{t+h} \leq x_t'\hat{\beta}_{\tau_{j+1}} \\ \phi(y_{t+h}|\hat{\mu_2}, \hat{\sigma}_2) & y_{t+h} > x_t'\hat{\beta}_{\tau_k}. \end{cases} \tag{25}$$

Algorithm 1, instead, relies on samples from the conditional density $\hat{f}_k(y_{t+h}|x_t)$, which lets us readily construct the whole density.

3 Simulation results

To evaluate the performance of the nonparametric approach to construction of the predictive density from QRs, relative to extant alternatives including the approach of ABG, we conduct a set of Monte Carlo experiments. These experiments let us assess the ability of the different approaches to uncover a range of distributional forms. We consider five data-generating processes (DGPs) that yield densities for $\{y_t\}_{t=1}^T$ that are:

1. (DGP1) Gaussian: $N(0,1)$.
2. (DGP2) Negatively skewed: $f(y;\mu=1,\sigma=2,\alpha=-0.5,\upsilon=10)$, where $f(.)$ is as defined in (7).
3. (DGP3) Skewness and high kurtosis: $f(y;\mu=1,\sigma=1,\alpha=1,\upsilon=5)$.
4. (DGP4) Bimodal (mixture of Gaussian) : $1/3N(0,.04)+2/3N(1,.04)$.
5. (DGP5) Trimodal (mixture of Gaussian): $1/6N(0,0.2)+1/3N(1,0.2)+1/2N(2,0.2)$.

For $\{y_t\}_{t=1}^T$ samples of size $T=100$ and $T=1,000$ drawn from each of these five DGPs, we then estimate six alternative densities and compare their fit against the (true) DGP density. In all cases, when estimating the QR, we set $x_t=1$, that is, we consider an intercept only.

The six densities we fit to the $\{y_t\}_{t=1}^T$ samples are:

1. NP(freq): estimate the QRs (where $k=19$, such that $\tau\in[0.05,0.10,...,0.90,0.95]$) using frequentist methods, (2), and then construct the density nonparametrically via Algorithm 1, setting $N=20,000$. We also experiment, as summarized below, with $k=4$ where $\tau\in[0.05,0.25,0.75,0.95]$ (as in ABG) and $k=99$ where $\tau\in[0.01,0.02,...,0.99]$.
2. EW(freq): estimate the QRs (where $k=19$, such that $\tau\in[0.05,0.10,...,0.90,0.95]$) using frequentist methods (as in NP(freq)) but then construct the density using equal weights, (23).
3. NP(B): estimate the QRs (where $k=19$, such that $\tau\in[0.05,0.10,...,0.90,0.95]$) using Bayesian methods and then construct the density nonparametrically via Algorithm 1. At the first stage, the Bayesian QR is estimated using a standard normal uninformative prior for the $q-$vector of β_τ coefficients, centered on a zero mean:

$$\beta_\tau \sim N(0, \mathbf{V}_\beta), \tag{26}$$

where $\mathbf{V}_\beta = 10\mathbf{I}_q$.

4. EW(B): estimate the QRs (where $k = 19$, such that $\tau \in [0.05, 0.10, ..., 0.90, 0.95]$) using Bayesian methods (as in NP(B)) but then construct the density using equal weights, (23).

5. ABG: follow ABG (using their replication material) and estimate the QRs (where $k = 4$, such that $\tau \in [0.05, 0.25, 0.75, 0.95]$) using frequentist methods and then construct the density parametrically via (7).[6]

6. ABG kernel: as a non-QR benchmark, follow ABG and nonparametrically estimate a kernel density.[7]

For all the Bayesian models, we estimate using 20,000 MCMC draws with a burn-in of 10,000 draws. Next, we then input each MCMC draw (across k quantiles) into Algorithm 1 and set $N = 100$. This delivers a vector of 1,000,000 draws from each predictive forecast density.

Tables 1 and 2, for $T = 100$ and $T = 1,000$, respectively, report the mean squared error (across 100 parallelized chains) of the first four moments of the fitted densities relative to the true (DGP) density and the average Kullback-Leibler (KL) distance between the fitted and true densities. KL is constructed as the expected difference in their logarithmic scores. Looking at the KL distance first, as a measure of overall density fit, we see that the nonparametric (NP) estimators, whether NP(freq) or NP(B), consistently deliver the better-fitting densities irrespective of the shape of the true density.[8] As anticipated, ABG's parametric approach is

[6]We note that in ABG's Matlab replication materials (available at `http://doi.org/10.3886/E113169V1`), when matching the quantile forecasts to the skewed-t density they approximate integrals with discrete sums. Specifically, looking at ABG's `Step2match.m` file (line 100), we see that they evaluate the skewed-t density only over a grid from -15 to 10. Instead, we use an exact analytical solution. In the empirical section below we return to this issue, showing its empirical importance.

[7]See equation (8) of ABG for details of the specific kernel density estimator employed.

[8]To isolate the role of k in explaining this result, given $k = 4$ in ABG but $k = 19$ in NP(freq), we experimented with NP(freq) when $k = 4$ ($\tau \in [0.05, 0.25, 0.75, 0.95]$) and $k = 99$ ($\tau \in [0.01, 0.02, ..., 0.99]$); and we experimented with ABG when k was increased from its maintained value of 4. As Table A1 in the online appendix shows, decreasing k to $k = 4$ markedly lessens the accuracy of NP(freq) and increasing k to $k = 99$ also worsens accuracy. While we might expect increases in k to improve accuracy for NP(freq), as the local uniformity assumption becomes weaker, parameter estimation errors increase for more extreme quantiles. The objective function of the standard QR estimator is not smooth, and the QR estimates can experience jumps. Future work might consider the benefits of producing the density forecasts having first smoothed the objective function, e.g., as in Fernandes, Guerre, and Horta (2021). Increasing k for NP(freq), well into the 5 percent tails as is the case when $k = 99$, was therefore found to deliver noisier estimates of the underlying conditional density, especially for the smaller $T = 100$. By contrast, due to its parametric assumption, increasing k did little to affect results for ABG.

competitive only when the true density is unimodal. Instabilities in estimation of the skewed-t density mean that ABG is not, however, always the best-fitting density even for DGP1 through DGP3, when the true density is unimodal, and we might expect the parametric nature of ABG to deliver gains. But for the multimodal densities (DGP4 and DGP5) use of Algorithm 1 is clearly preferable, whether deployed on a QR estimated by frequentist or Bayesian methods: both NP(freq) and NP(B) are consistently the best performers in terms of delivering the lower KL values. The NP algorithms also match ABG for the unimodal densities (DGP1 through DGP3). The equal-weighted (EW) approaches, as expected, do not produce as low KL values as NP does, but they again outperform ABG for DGP4 and DGP5. There is some evidence that EW(B), because of the extra parameter estimation uncertainty that is accommodated, yields more volatile estimates than EW(freq). In contrast, the extra smoothing involved means this result does not hold for NP. The benchmark ABG kernel density, like the NP estimators, can also accommodate multimodalities. However, the kernel density does not deliver as good-fitting densities as the NP approaches, in particular for the smaller sample size of $T = 100$.

Turning to the accuracy of the first four moments, as judged by the mean squared error (MSE) between the respective moment of the fitted and true densities, we again see that the NP estimators tend to be more accurate than ABG and kernel. The EW approach can also be competitive, although accuracy for the unimodal densities (DGP1 through DGP3) can deteriorate, particularly when the QRs are estimated by Bayesian methods. We attribute this to the inability of EW to provide as smooth a representation of the tails of the density as NP. We also note how explosive estimation, for some Monte Carlo replications, pushes up the MSE estimates in some instances, especially for EW(B) and ABG. When estimates of $\upsilon < 4$, not all of the first four moments of the skewed-t density are defined.

In sum, the Monte Carlo evidence confirms that the choice of how to fit a density to quantile forecasts matters. While ABG's parametric assumption may work well, unsurprisingly it will only do so for true densities that are unimodal. Instead, it is relatively simple to let the "data speak," as they do when estimating the QRs in the first place, and use nonparametric approaches as detailed in Algorithm 1 to construct the forecast density from the quantile forecasts. While these simulations are, of course, just illustrative, they do indicate how the nonparametric approach of Algorithm 1 can flexibly accommodate a greater variety of distributional shapes than ABG, even for modest sample sizes. They also suggest that when using Algorithm 1 intermediate values of k (such as $k = 19$) best approximate the underlying density.

In principle, we anticipate a trade-off when selecting what k to use in Algorithm 1. Too small a value does not give NP sufficient flexibility to smoothly fit different distributional shapes. Too large a value for k, especially for smaller sample sizes, T, increasingly forces the

QR into the tails of the density, where there are fewer observations. This may induce noise in the forecast density, and it raises the risk of introducing erroneous spikes or modes (under-smoothing) in the forecast density when fitted using NP. To investigate this possible trade-off, in the online appendix we report supplementary simulation results (see Table A2). These involve, for DGP1 through DGP5, using the calibrated unimodality test of J. A. Hartigan and P. M. Hartigan (1985), as proposed by Cheng and Hall (1998), and reporting the proportion of rejections of unimodality. Table A2 confirms that while increasing k, when using NP(freq), does increase the chance of identifying false peaks in the unimodal densities of DGP1 through DGP3, this risk rapidly declines to zero for sample sizes of $T > 50$. This suggests that increasing k does not inject false peaks into the fitted densities, except for very small samples ($T = 25$). In turn, for the multimodal DGPs (DGP4 and DGP5), NP(freq) does a good job of rejecting unimodality, except for smaller values of k (specifically, $k = 4$ and $k = 9$). As long as k is at least 19, we see rejection rates in Table A2 of over 90 percent, even when $T = 25$. These rejection rates rise further as T increases. In short, these supplementary unimodality tests both support the use of intermediate values of k when using Algorithm 1 and provide confidence that Algorithm 1 does not identify false modes in the forecast density, unless T is especially small relative to k.

Table 1: Average Mean Squared Error and Kullback-Leibler (KL) distance for $T = 100$

Models	Mean	Variance	Skewness	Kurtosis	KL
DGP1: Unimodal (Gaussian)					
NP(freq)	0.01	0.03	0.12	0.40	0.02
EW(freq)	0.01	0.02	0.12	0.38	0.01
NP(B)	0.01	0.03	0.10	0.79	0.04
EW(B)	0.01	0.07	0.03	0.45	0.12
ABG	0.01	0.05	Inf	Inf	0.02
ABG Kernel	0.01	0.07	0.04	0.10	0.02
DGP2: Unimodal (Negative Skewness)					
NP(freq)	0.05	0.73	0.14	1.51	0.02
EW(freq)	0.04	0.68	0.13	1.48	0.01
NP(B)	0.05	0.67	0.13	1.00	0.05
EW(B)	0.04	1.81	0.05	2.67	0.10
ABG	0.05	Inf	Inf	Inf	0.03
ABG Kernel	0.05	1.32	0.10	0.82	0.04
DGP3: Unimodal (Skewness & High Kurtosis)					
NP(freq)	0.01	0.12	1.11	80.41	0.02
EW(freq)	0.01	0.10	1.06	79.44	0.00
NP(B)	0.01	0.08	0.49	51.28	0.05
EW(B)	0.01	0.24	0.62	84.51	0.10
ABG	0.01	Inf	Inf	Inf	0.03
ABG Kernel	0.01	0.30	0.66	59.62	0.12
DGP4: Bimodal					
NP(freq)	0.00	0.00	0.01	0.04	0.03
EW(freq)	0.00	0.00	0.01	0.03	0.11
NP(B)	0.00	0.00	0.01	0.05	0.04
EW(B)	0.00	0.00	0.01	0.01	0.13
ABG	0.00	0.00	0.30	6.14	0.30
ABG Kernel	0.00	0.00	0.01	0.11	0.11
DGP5: Trimodal					
NP(freq)	0.00	0.00	0.01	0.04	0.05
EW(freq)	0.00	0.00	0.01	0.05	0.36
NP(B)	0.00	0.00	0.01	0.09	0.05
EW(B)	0.00	0.01	0.01	0.02	0.14
ABG	0.00	0.01	0.31	5.20	0.26
ABG Kernel	0.00	0.01	0.02	0.07	0.21

Notes: Inf denotes infinity. NP(freq) uses $k = 19$. The 6 estimators and 5 DGPs are defined in Section 3.

Table 2: Average Mean Squared Error and Kullback-Leibler (KL) distance for $T = 1,000$

Models	**Mean**	**Variance**	**Skewness**	**Kurtosis**	**KL**
DGP1: Unimodal (Gaussian)					
NP(freq)	0.00	0.01	0.06	0.15	0.00
EW(freq)	0.00	0.01	0.05	0.17	0.00
NP(B)	0.00	0.00	0.01	0.08	0.01
EW(B)	0.00	0.06	0.00	0.53	0.06
ABG	0.00	0.00	0.02	0.21	0.00
ABG Kernel	0.00	0.01	0.01	0.02	0.01
DGP2: Unimodal (Negative Skewness)					
NP(freq)	0.01	0.31	0.06	1.04	0.00
EW(freq)	0.01	0.33	0.06	1.09	0.00
NP(B)	0.00	0.08	0.02	0.42	0.01
EW(B)	0.00	1.94	0.02	2.74	0.12
ABG	0.00	0.15	0.04	Inf	0.00
ABG Kernel	0.00	0.18	0.02	0.30	0.01
DGP3: Unimodal (Skewness & High Kurtosis)					
NP(freq)	0.00	0.10	0.99	82.64	0.00
EW(freq)	0.00	0.10	1.03	82.04	0.01
NP(B)	0.00	0.02	0.25	56.39	0.01
EW(B)	0.00	0.25	0.56	86.42	0.05
ABG	0.00	0.03	Inf	Inf	0.00
ABG Kernel	0.00	0.03	0.60	142.25	0.05
DGP4: Bimodal					
NP(freq)	0.00	0.00	0.00	0.00	0.00
EW(freq)	0.00	0.00	0.00	0.00	0.11
NP(B)	0.00	0.00	0.00	0.05	0.02
EW(B)	0.00	0.00	0.00	0.01	0.08
ABG	0.00	0.00	0.32	6.23	0.31
ABG Kernel	0.00	0.00	0.00	0.02	0.03
DGP5: Trimodal					
NP(freq)	0.00	0.00	0.00	0.01	0.03
EW(freq)	0.00	0.00	0.00	0.01	0.36
NP(B)	0.00	0.00	0.00	0.03	0.03
EW(B)	0.00	0.00	0.00	0.00	0.06
ABG	0.00	0.01	0.30	5.09	0.25
ABG Kernel	0.00	0.00	0.00	0.01	0.09

4 Empirical results: Revisiting the growth-at-risk application of ABG

ABG established the empirical utility of quantile regressions for modeling and particularly forecasting the conditional density of US GDP growth. They found that deteriorating financial conditions, as captured by the Chicago Fed's National Financial Conditions Index (NFCI), have an asymmetric effect on GDP growth.[9] In particular, they link GDP growth tail risks to poor financial conditions. Recessions are associated with left-skewed conditional forecast densities. Carriero, Clark, and Marcellino (2023) challenge this view, noting that ABG's empirical finding that downside risk varies more than upside risk could equally well be explained by symmetric conditional forecast densities as by asymmetric unconditional forecast densities. These could be produced, for example, by Bayesian VAR models with stochastic volatility. Caldara et al. (2021) similarly suggest use of a parametric modeling framework that rationalizes the empirical findings of ABG but maintains use of symmetric conditional densities. They capture nonlinear effects with a Markov-switching model, in which the transition probabilities depend, *inter alia*, on financial conditions. This fits with a long literature supportive of nonlinear models of GDP growth, notably Hamilton (1989), that finds GDP growth is well characterized as regime-switching. Such regime-switching models imply unconditional multimodality. But while they usually imply conditional (within a regime) unimodality, if a QR were fitted to data generated from a regime-switching model the conditional densities from the QR need not be unimodal.[10] Adrian, Boyarchenko, and Giannone (2021) also jettison the use of QR and instead use kernel-based estimators to support their finding that the forecast density of GDP growth is approximately Gaussian and unimodal during normal periods, but becomes multimodal during periods of tight financial conditions. They also make the theoretical case for multimodality, explaining how it arises in macrofinancial intermediary models with occasionally binding financial constraints.

Given the degree to which ABG's empirical findings, based on their parametric quantile-matching approach, have influenced the subsequent literature, as we have just selectively reviewed, we emphasize the importance of letting the "data speak" about the nature of the conditional density forecast for GDP growth when mapping the quantile forecasts to the density forecasts. Accordingly, we revisit ABG's application. But we compare their skewed-t

[9] The NFCI aggregates a large set of variables capturing credit quality, risk, and leverage.

[10] More generally, we emphasize that observational equivalence in reduced-form relationships is consistent with rival structural explanations. As a motivating example in another applied context, Benati and Surico (2009) show how rival structural explanations for the Great Moderation are consistent with the (same) reduced-form evidence. So while ABG established that QRs evidence a nonlinear relationship between GDP growth and financial conditions, as a nonparametric (reduced-form) tool QRs cannot discriminate between alternative more structural explanations for the drivers of GDP growth.

conditional density forecasts, which assume unimodality but allow for asymmetry, with those conditional density forecasts formed when we make no such assumption and, via Algorithm 1, better let the data inform this mapping.

Specifically, to facilitate comparison with ABG's parametric approach to constructing forecast densities from QRs, we use their data, sample periods, and preferred models. Specifically, we estimate QR models relating GDP growth to both lagged GDP growth and the NFCI.[11] This then lets us produce, via the aforementioned parametric and nonparametric approaches, one-quarter-ahead and one-year-ahead forecast densities for GDP growth conditional first on both lagged GDP growth and the NFCI and second on just lagged GDP growth. Thereby, we isolate the role that the NFCI plays in driving results. We re-assess ABG's claim that financial conditions are critical when density forecasting GDP growth in the US. In common with much of the literature, we focus on assessing the in-sample fit of the conditional densities. Thus we provide guidance on the importance of considering how to fit a density to the quantile forecasts. But we do provide some out-of-sample evaluation evidence too, although the latter arguably tells us more about the instabilities faced out-of-sample (see Rossi (2021)) than about the relative merits of different ways of constructing predictive densities from QRs. Nevertheless, in anticipation of the known benefits of shrinkage when forecasting out-of-sample, we do consider a variant of NP(B) that imposes a more informative prior. That is, we estimate Bayesian QRs with Minnesota priors. We follow Carriero, Clark, and Marcellino (2022) and set V_i, the i-diagonal elements of $\mathbf{V}_\beta$, as follows:

$$V_i = \begin{cases} \lambda_1 \lambda_2 \frac{\sigma_{GDP}}{\sigma_j} & \text{for the coefficients other than the lag } l \text{ of GDP,} \\ \frac{\lambda_1}{l^{\lambda_3}} & \text{for the coefficients on the lag } l \text{ of GDP,} \\ 1000\sigma_{GDP} & \text{for the intercept,} \end{cases} \tag{27}$$

where σ_{GDP} and σ_j are the standard deviations from an AR(4) model for GDP growth and the j-th regressor (other than GDP growth), estimated with data available at the forecast origin. We follow Carriero, Clark, and Marcellino (2022) and set $\lambda_1 = \lambda_2 = 0.2$, and $\lambda_3 = 1$. In terms of the in-sample fit, the prior variance on the coefficient on the lag of GDP is 0.2 for both the one-quarter- and one-year-ahead forecasts. On the other hand, the prior variance on

[11] A subsequent literature has also used QRs to model GaR and construct GDP growth density forecasts. But it has examined the benefits of disaggregating the Chicago Fed's NFCI, using real-time NFCI vintages, and/or considered additional indicators; e.g., see Plagborg-Moller et al. (2020), Reichlin, Ricco, and Hasenzagl (2020), Brownlees and Souza (2021), Kohns and Szendrei (2021), and Amburgey and McCracken (2023). Given the importance of the original modeling strategy in shaping the ongoing research agenda, as summarized in our introduction, we return to ABG's model space and consider (latest-vintage) NFCI alone. We expect that adding in extra variables and allowing for possible additional nonlinearities will further distinguish our approach from ABG's. Given their skewed-t assumption, ABG's densities cannot accommodate the likely multimodalities associated with nonlinearity.

the coefficient for the NFCI differs. One-quarter-ahead, its prior variance is 0.25, while one-year-ahead it is 0.08. Let NP(BM) denote forecast densities produced using this Minnesota prior and Algorithm 1.

Given this paper's emphasis on construction of the entire predictive density rather than just estimating GaR, we focus on assessing the overall fit of the competing forecast densities using probability integral transforms (PITs), i.e., the CDF of the forecast evaluated at the subsequent realization of GDP growth. For correctly calibrated forecast densities (see Diebold, Gunther, and Tay (1998) and Mitchell and Wallis (2011)), these PITs, at the minimum, should be uniformly distributed. As shown by Diebold, Gunther, and Tay (1998), correctly calibrated forecast densities will be preferred by all users, irrespective of their loss function. Specifically, we use the Rossi and Sekhposyan (2019) test and, following their recommendation, for multi-step-ahead forecasts, given the serial correlation in the PITs, to construct the critical values we use a block bootstrap of length $P^{1/3}$, where P is the sample size in the evaluation period. Nevertheless, to supplement these PITs-based tests of calibration and to facilitate cross-model comparison, we also report two commonly used scoring rules for density evaluation: the average logarithmic predictive score and the average continuous ranked probability score (CRPS). The CRPS is a popular density forecast-based scoring rule that offers greater robustness to outliers than the logarithmic score used by ABG; see Gneiting and Raftery (2007). We also looked at forecast accuracy in specific regions of the forecast density, using the PITs-based test of Rossi and Sekhposyan (2019) and the quantile-weighted CRPS of Gneiting and Ranjan (2011); these results are summarized below, drawing on the tables in the online appendix.

Figures 2 and 3 plot the cumulated PITs, respectively, for the one-quarter-ahead and one-year-ahead forecast densities produced using the models of Section 3 plus NP(BM).[12] These models consider both the NFCI and lagged GDP growth as conditioning information, as favored by ABG. We also plot the PITs dropping the NFCI from the QR, to isolate the importance of conditioning on financial conditions when density forecasting GDP growth.[13] Looking at these cumulated PIT plots across these two figures, it is apparent that both of the new approaches (NP and EW), whether estimated by frequentist or Bayesian methods, deliver better calibrated forecast densities than either ABG or ABG kernel. Their cumulated PITs are closer to the 45-degree line. While based on the same frequentist QR as in ABG, this indicates that fitting the skewed-t density to these same quantile forecasts is not as beneficial as using Algorithm 1 or indeed using EW. To investigate whether it is the higher value of

[12]We drop EW(freq) to make space for NP(BM), noting that results using EW(freq), as in the Monte Carlo, are in general slightly worse than those using NP(freq).

[13]We emphasize how when constructing the ABG densities we use ABG's replication code. Therefore, as discussed in Section 3, we approximate integrals with discrete sums. We return later to the empirical applications of this.

$k = 19$ in NP(freq), relative to ABG (where $k = 4$), that explains this result rather than the use of Algorithm 1, we produced predictive densities from ABG assuming $k = 19$ (see Figure A5 in the online appendix). As in the Monte Carlo experiments, these alternative ABG densities are found to perform similarly to those when $k = 4$. Thus, we conclude that it is the use of Algorithm 1, rather than a different sized k, that yields the forecasting gains. But the ABG densities are still well-calibrated, since while we do observe a few extra little deviations from the 45-degree line, their cumulated PITs still remain well within the critical value bands. Interestingly, all densities are well-calibrated at a 95 percent significance level, according to the PITs test of Rossi and Sekhposyan (2019), irrespective of whether the NFCI is included in the QR.[14]

Figure 2: CDF of the in-sample PITs (one-quarter-ahead forecasts, 1973Q1-2015Q4) from the 6 density forecasts with and without the NFCI

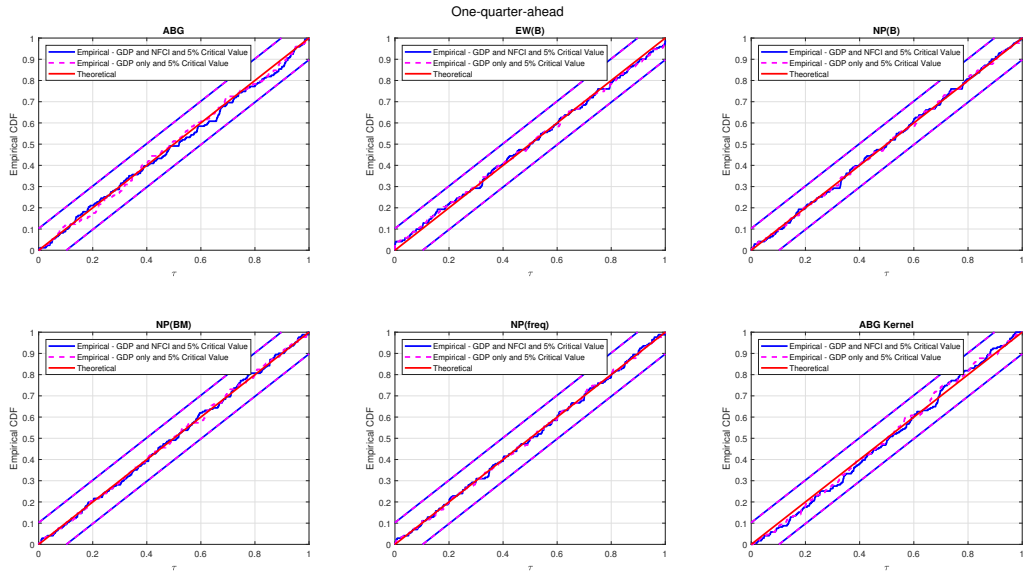

Notes: The 5 estimators (ABG, EW(B), NP(B), NP(freq), and ABG Kernel) are defined in Section 3. NP(BM) uses the nonparametric Algorithm 1 and estimates a Bayesian QR with the Minnesota prior of Carriero, Clark, and Marcellino (2022). The figures show the empirical CDF of the PITs (blue line) from the QR models with the NFCI (and lagged GDP), the empirical CDF of the PITs (dashed red line) from the QR models without the NFCI, the CDF of the PITs under the null hypothesis of correct calibration (the 45-degree line), and the 5% critical value bands of the Rossi and Sekhposyan (2019) PITs test.

[14]Figure A6 in the online appendix again shows how the choice of k in NP(freq) matters. From the S-shaped nature of the cumulated PITs, we can infer that the density forecast is too narrow at $k = 4$. Calibration is better at $k = 99$, but not obviously better than when $k = 19$ (as shown in Figures 2 and 3). This is consistent with the Monte Carlo evidence in Section 3 that a "medium-sized" value for k appears sufficient. The critical value bands of Rossi and Sekhposyan (2019) should be taken as "general guidance," to quote ABG, since they are derived assuming a rolling window of estimation, while, like ABG, we use an expanding window.

Figure 3: CDF of the in-sample PITs (one-year-ahead forecasts, 1973Q4-2015Q4) from the 6 density forecasts with and without the NFCI

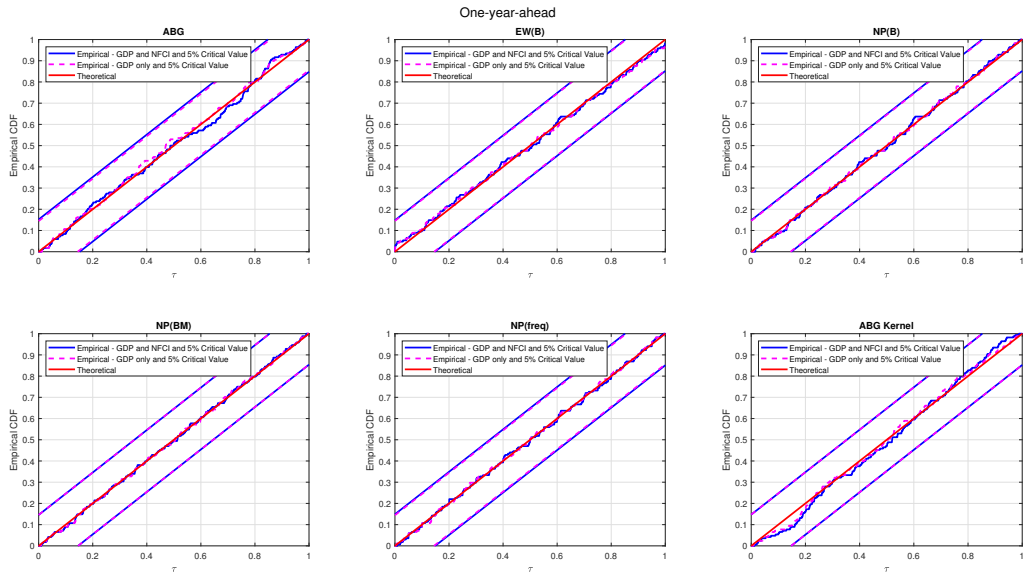

Notes: See notes to Figure 2.

Figure 4 confirms that using one of our preferred densities, we take NP(freq), when conditioned on both the NFCI and lagged GDP growth, does not change the central narrative of ABG: the left tail of the conditional density of GDP growth moves with the tightness of financial conditions.[15] And the right tail is relatively invariant. Figure 4 evidences this by plotting, over time, the expected shortfall and longrise estimates from both ABG and NP(freq). Expected shortfall (SF_{t+h}) and longrise (LR_{t+h}) summarize downside and upside risk, respectively. They measure the total probability mass that the conditional distribution assigns to the left and right tails of the distribution:

$$SF_{t+h} = \frac{1}{\pi}\int_{0}^{\pi} \hat{F}^{-1}_{y_{t+h}|x_t}(\tau|x_t)d\tau; \tag{28}$$

$$LR_{t+h} = \frac{1}{\pi}\int_{1-\pi}^{1} \hat{F}^{-1}_{y_{t+h}|x_t}(\tau|x_t)d\tau. \tag{29}$$

Figure 4 shows that the expected shortfall and longrise estimates from ABG and NP(freq) track each other very closely. Expected shortfall is far more volatile than expected longrise, as the narrative of ABG emphasizes.

[15]This "stylized fact" has been confirmed using alternative modeling approaches to QR, such as the parametric time-varying skewed-t model of Delle Monache, De Polis, and Petrella (2023).

Figure 4: In-sample plots of the expected shortfall and expected longrise at $\tau = 0.05$ using ABG and NP(freq), from QRs with the NFCI and lagged GDP

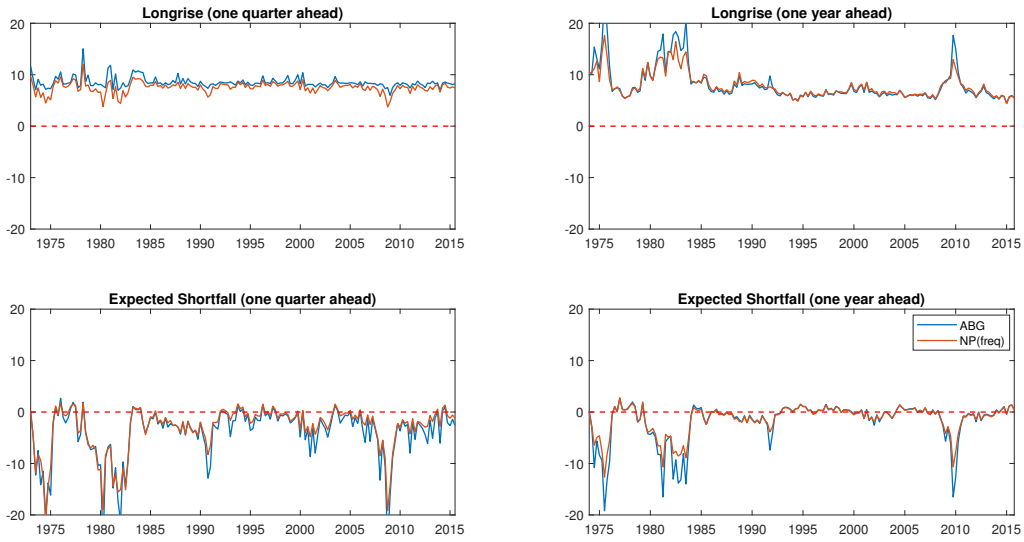

However, despite this similarity, when we look more deeply at the densities underlying these estimates we start to appreciate that the choice of how to construct the density from the quantile forecasts does still matter. It can reveal further features of economic interest. Figures 5 and 6 show this by plotting, over time, for the one-quarter-ahead and one-year-ahead forecasts, respectively, the first 4 moments of the ABG and NP(freq) densities. While the first two moments from ABG and NP(freq) are similar, the third and especially fourth moments differ, albeit they share some commonalities. In particular, we note how the evidence for or against skewness in GDP growth varies over time. This is consistent with Carriero, Clark, and Marcellino (2023), who find, using alternative tests, weak evidence for skewness. Figure 5, in particular, shows that NP(freq) points to less negative skewness during the period of the global financial crisis.[16] This disagreement between ABG and NP(freq) is also consistent with the finding in Plagborg-Moller et al. (2020) that only the lower moments of the GDP growth conditional density are well-estimated.[17]

Next we provide some illustrative in-sample plots of our predictive densities. In Figure 7 we zoom in on a relatively stable period: 2005. Then, in Figure 8, we look at 2008, during the global financial crisis, a period also emphasized in ABG and Adrian, Boyarchenko, and

[16]This is consistent with modest falls in the degree of asymmetry when NP(freq) rather than ABG is used in Figure 4. That is, while following the same general patterns, expected shortfall and longrise are more volatile, over time, when ABG rather than NP(freq) is consulted.

[17]Figures A7 and A8 in the online appendix indicate how ABG's coding choice to assess the skewed-t density over a finite grid is important. If, instead, we assess the skewed-t density analytically, instead of relying on ABG's approximation, we observe far more extreme estimates for the higher moments.

Figure 5: In-sample plots of the four moments of the ABG and NP(freq) forecast densities (one-quarter-ahead), from QRs with the NFCI and lagged GDP

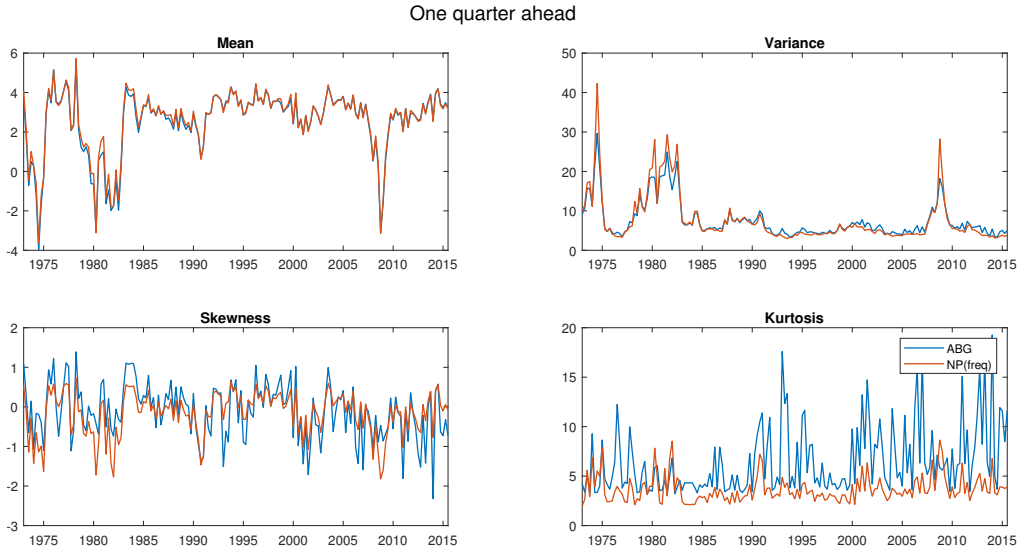

Giannone (2021). We focus on the one-quarter-ahead in-sample densities, with the analogous one-year-ahead and out-of-sample plots in the online appendix.[18] Confirming the findings of Adrian, Boyarchenko, and Giannone (2021), who use kernel methods, clear evidence of multimodality emerges at the time of the global financial crisis when we use Algorithm 1 to construct the density forecast from the QR.[19] If, as in ABG, we assume a skewed-t density we obscure this important macroeconomic feature. Instead, we would simply infer more evidence for a skewed density. The evidence of multimodality during the global financial crisis, gleaned from NP(freq), is somewhat more muted when we look at the out-of-sample density forecasts as plotted in the online appendix. But, as shown by Figure 9, when the calibrated unimodality test of J. A. Hartigan and P. M. Hartigan (1985) as proposed by Cheng and Hall (1998) is used, rejections of unimodality are far greater when we do condition on the NFCI. These rejections are especially pronounced during NBER recessionary periods, again confirming the finding of Adrian, Boyarchenko, and Giannone (2021). We do also see evidence from these unimodality

[18]Figures A11 through A16 in the online appendix qualitatively confirm the impression from Figures 7 and 8.

[19]There is also recent evidence that professional forecasters' density forecasts for GDP growth are best acknowledged, at certain points in time, as multimodal. Ganics, Rossi, and Sekhposyan (2023), who study the Survey of Professional Forecasters in the US, find that multimodalities in their combined GDP growth densities emerge around business cycle turning points, such as the Great Recession. Figures A21 and A22 in the online appendix (Section A.5) illustrate that while decreasing k does, as anticipated, affect the look of the forecast densities, increasing k does not. This offers some reassurance, further to the aforementioned simulation evidence in Table A2 in the online appendix, that our evidence for multimodality is not a direct consequence of setting $k = 19$.

Figure 6: In-sample plots of the four moments of the ABG and NP(freq) forecast densities (one-year-ahead), from QRs with the NFCI and lagged GDP

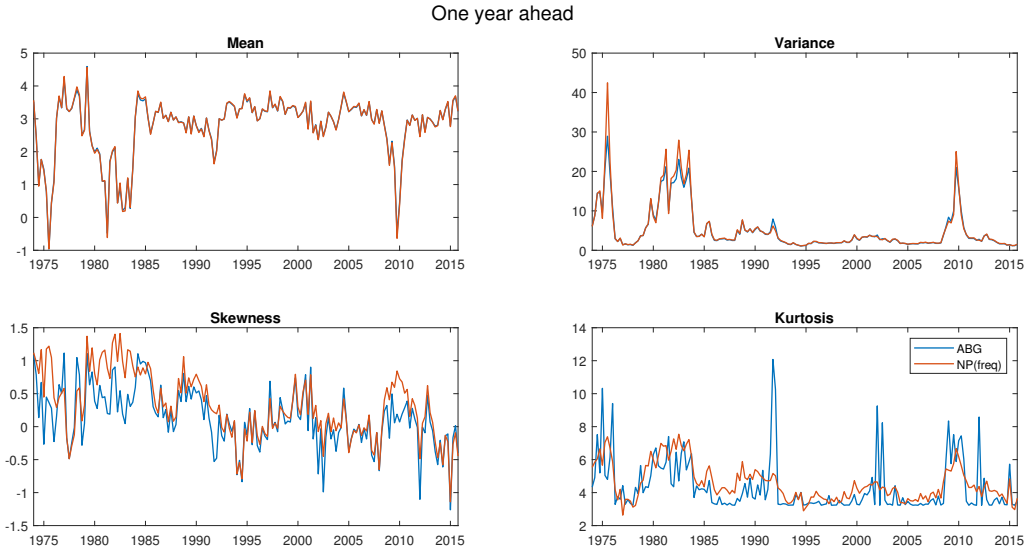

tests that the properties of the GDP growth density change quite rapidly, even outside of recessionary periods, especially when conditioning on the NFCI. As we go on to discuss next, this may be explained by the NFCI being a weak predictor, so that small movements in the NFCI can lead to (larger) changes in the shape of the predictive densities for GDP.

We should emphasize, however, that these empirical features may well be a product of the predictors (the model space) chosen to explain GDP growth. To facilitate direct comparison with ABG and draw out the empirical relevance of their choice to assume a skewed-t density, our application uses their two predictors: lagged GDP growth and the NFCI. An interpretation of our (and ABG's) results is that we see the longer left tails to the GDP growth density emerge during recessions as the NFCI pushes the low conditional quantiles to the left while leaving the rest of the distribution relatively unaffected. If additional - and importantly *better* - predictors of GDP growth were considered, one could imagine that the center of the forecast density would also shift to the left during recessions. Thus, rather than see recessions associated with longer left tails, we would simply observe the whole forecast density shift to the left. To begin to investigate this claim empirically, we experimented with expanding our set of predictors to consider the global and financial factors suggested by Plagborg-Moller et al. (2020). As summarized in the online appendix (Section A.6), this expanded set of predictors delivers more accurate density forecasts. It also results in forecast densities that look more symmetric over recessions, although evidence of multimodality remains.

Finally, we turn to out-of-sample evaluation of the forecast densities over the sample period

Figure 7: GDP growth density forecasts conditional on the NFCI and lagged GDP for 2005 made one-quarter-ahead (in-sample)

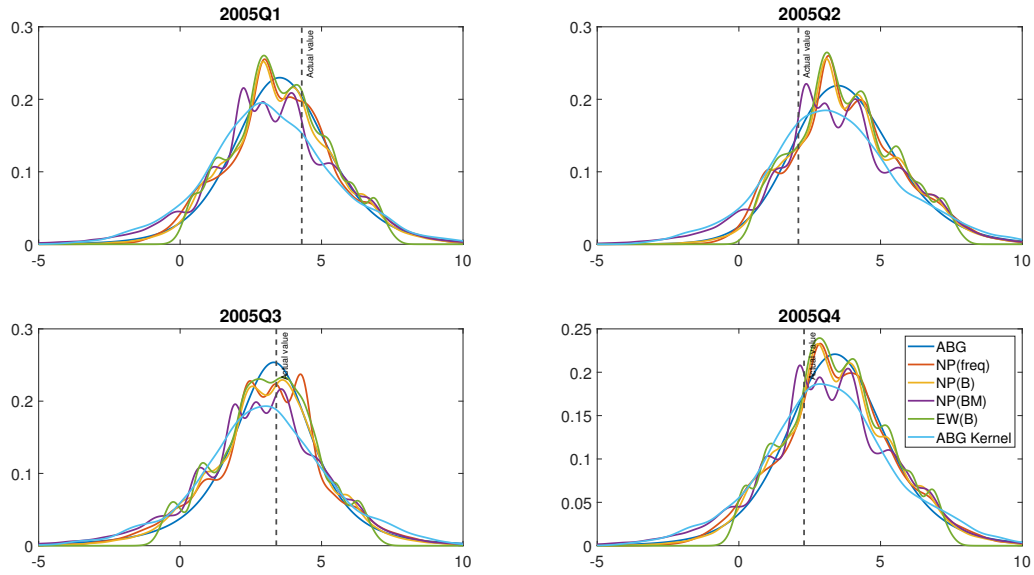

Notes: The 5 estimators (ABG, NP(freq), NP(B), EW(B), and ABG Kernel) are defined in Section 3. NP(BM) uses the nonparametric Algorithm 1 and estimates a Bayesian QR with the Minnesota prior of Carriero, Clark, and Marcellino (2022).

Figure 8: GDP growth density forecasts conditional on the NFCI and lagged GDP for 2008 made one-quarter-ahead (in-sample)

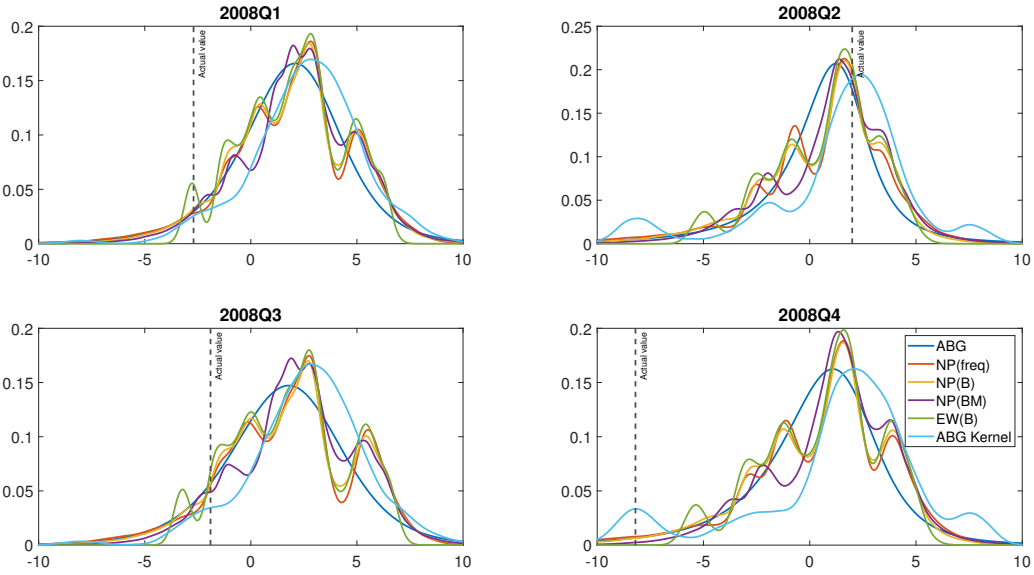

Figure 9: P-values over time from the calibrated Hartigans' unimodality test

Panel A: NFCI and GDP

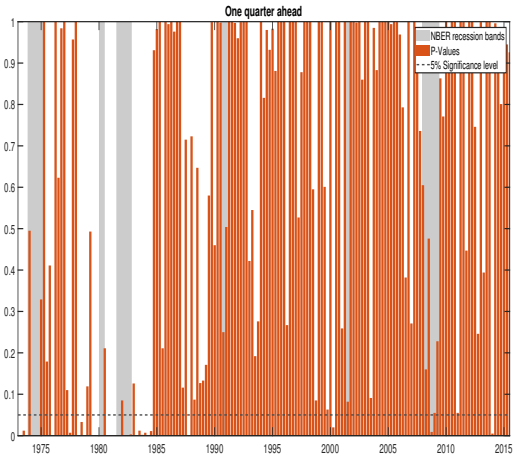

Panel B: NFCI and GDP

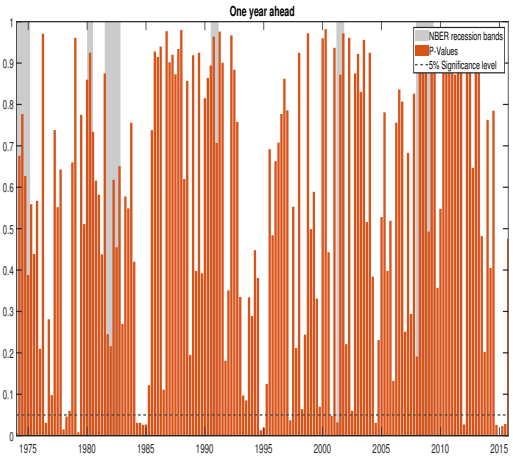

Panel C: GDP only

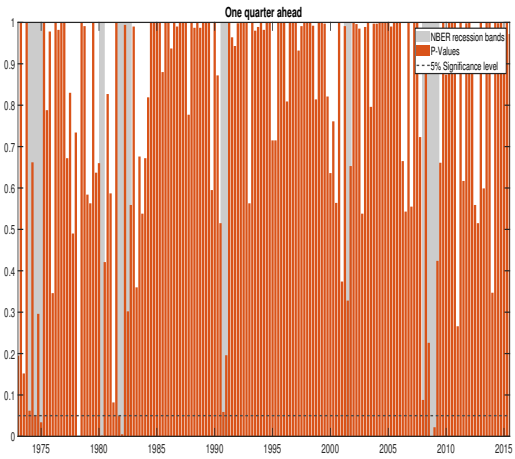

Panel D: GDP only

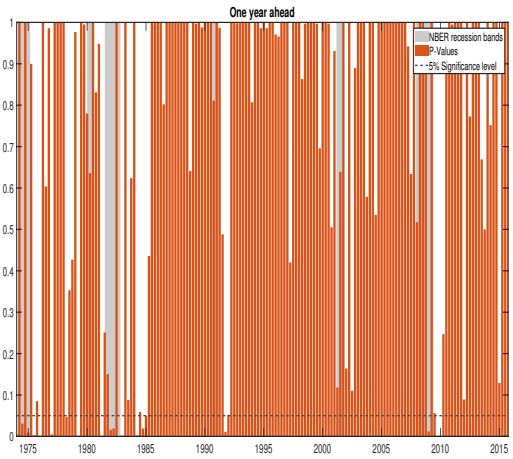

Notes: Panel A reports the p-values from the Hartigans' unimodality test (one-quarter-ahead) for the NP(freq) in-sample GDP growth density forecasts conditional on the NFCI and lagged GDP. Panel B reports the p-values from the Hartigans' unimodality test over time (one-year-ahead) for the NP(freq) in-sample GDP growth density forecasts conditional on the NFCI and lagged GDP. Panel C reports the p-values from the Hartigans' unimodality test over time (one-quarter-ahead) for the NP(freq) in-sample GDP growth density forecasts conditional on only lagged GDP. Panel D reports the p-values from the Hartigans' unimodality test over time (one-year-ahead) for the NP(freq) in-sample GDP growth density forecasts conditional only on lagged GDP. NBER recessionary periods are shaded gray.

1993Q1-2015Q4. Again this is the same evaluation period as in ABG, and we follow ABG in recursively producing the predictive densities from QRs estimated on expanding windows of data dating back to 1973Q1. Figures 10 and 11 show that the accuracy of the forecast densities is, as expected, considerably worse out-of-sample. Comparison with the in-sample densities indicates that they too deteriorate in accuracy when evaluated on the sub-sample from 1993.[20] ABG does especially poorly, with the null hypothesis of correct calibration rejected at a 95 percent significance level both one-quarter- and one-year-ahead. By contrast, the cumulated PITs are closer to the 45-degree line when Algorithm 1 is used on a QR estimated by Bayesian methods with the Minnesota prior: NP(BM). Figures 10 and 11 also show that across methods the PITs are closer to the 45-degree line when not conditioning on financial conditions, reminding us that autoregressive models can be hard to beat when forecasting out-of-sample.

Figure 10: CDF of the out-of-sample PITs (one-quarter-ahead, 1993Q1-2015Q4) from the 6 density forecasts with the NFCI and lagged GDP

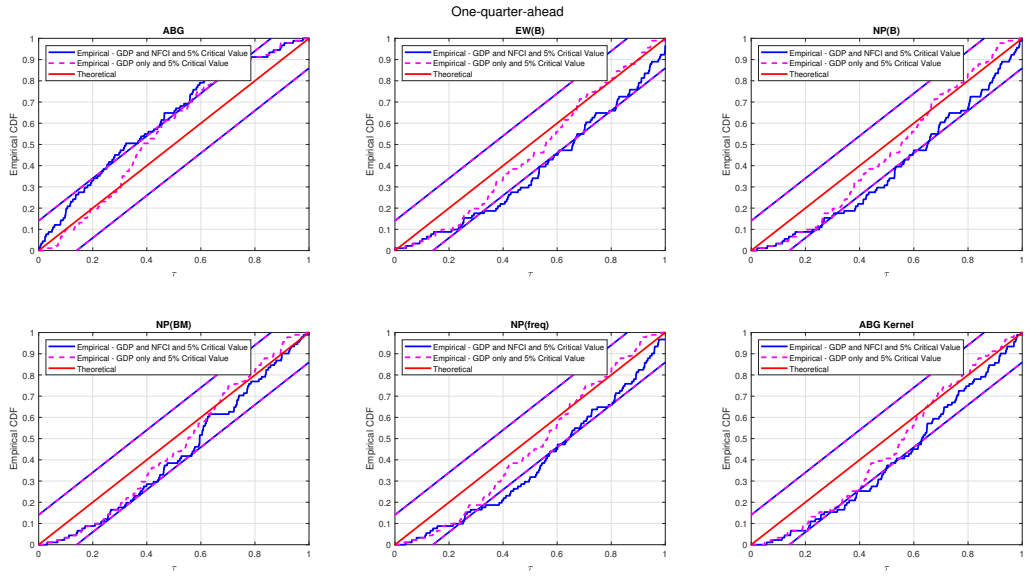

Notes: The figures show the empirical CDF of the PITs (red line), the CDF of the PITs under the null hypothesis of correct calibration (the 45-degree line), and the 5% critical value bands of the Rossi and Sekhposyan (2019) PITs test. The 5 estimators (ABG, NP(freq), NP(B), EW(B), and ABG Kernel) are defined in Section 3. NP(BM) uses the nonparametric Algorithm 1 and estimates a Bayesian QR with the Minnesota prior of Carriero, Clark, and Marcellino (2022).

Table 3 shows that out-of-sample the Bayesian QR methods with the Minnesota prior using Algorithm 1 (NP(BM)) deliver the highest average logarithmic predictive scores and the lowest CRPSs when conditioning on the NFCI. But the average logarithmic score statistics,

[20] See Figures A9 and A10 in the online appendix.

Figure 11: CDF of the out-of-sample PITs (one-year-ahead, 1993q4-2015Q4) from the 6 density forecasts with the NFCI and lagged GDP

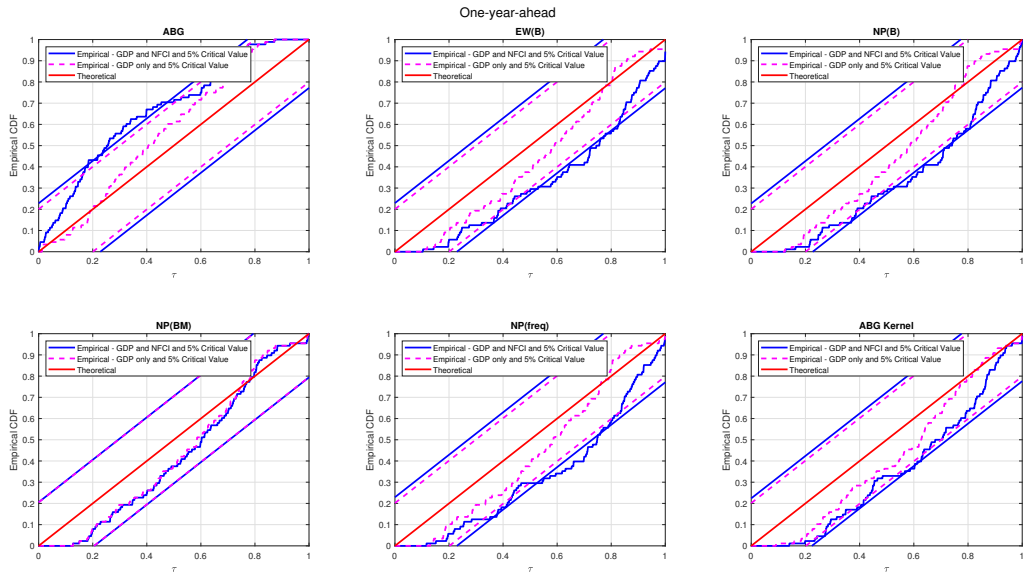

Notes: See notes to Figure 10.

in particular, are dominated by the forecasting failures at the time of the global financial crisis.[21] So we prefer to emphasize the CRPS, given that it is more robust to large but rare forecasting errors.[22] Conditioning the GDP density forecasts on the NFCI also tends to lead to improvements in the CRPS, especially one-quarter-ahead. Importantly, in terms of this paper's focus on isolating the best means of constructing density forecasts from the same quantile forecasts, Table 3 shows that NP at least matches the accuracy of ABG, at both forecast horizons.

Despite the fact that the accuracy of the ABG densities is often improved upon, both in-sample and out-of-sample, this is not the key takeaway we wish to emphasize. Instead, the bottom line is that these alternative nonparametric ways of constructing the predictive density from QRs *on average* match, and at times (albeit perhaps modestly) improve upon, the statistical accuracy of the ABG densities.[23] But in so doing they unmask deviations from

[21] Figures A19 and A20 in the online appendix demonstrate this by plotting the quarter-by-quarter log scores. EW(B) does especially poorly over the recession.

[22] When we use the Rossi and Sekhposyan (2019) test to assess the calibration of specific regions of the forecast distribution, we see even more clearly how NP(BM) provides more accurate forecasts than ABG in the upper right half of the forecast density, with ABG also bettered in the left tail but less strongly; see Table A5 in the online appendix. The cross-model differences in the quantile-weighted CRPS statistics reported in Table A6, however, appear more modest, although ABG is still beaten.

[23] Giacomini and White (2006) tests confirm that the differences between the average scores seen in Table 3 are not statistically significant at traditional significance levels.

Table 3: Average log predictive score (LPS) and continuous ranked probability score (CRPS) for the one-quarter-ahead forecasts (out-of-sample, 1993Q1-2015Q4) and the one-year-ahead forecasts (out-of-sample, 1993Q4-2015Q4)

	With NFCI & GDP				With lagged GDP only			
	One-quarter-ahead		One-year-ahead		One-quarter-ahead		One-year-ahead	
	LPS	CRPS	LPS	CRPS	LPS	CRPS	LPS	CRPS
ABG	-2.24	1.27	-2.02	0.98	-2.31	1.32	-1.99	0.96
EW(B)	-0.81	0.98	-1.27	0.99	-0.36	0.97	-1.06	0.98
NP(B)	-0.01	0.98	0.02	0.99	0.00	0.98	-0.03	1.00
NP(BM)	0.01	0.98	0.01	0.98	0.00	0.98	-0.03	1.00
NP(freq)	-0.23	0.99	-0.03	0.99	-0.02	0.98	-0.09	1.00
ABG Kernel	-0.03	1.03	-0.09	1.04	-0.03	1.00	-0.11	1.03

Notes: The LPS values are presented relative to (by subtraction of) the LPS from ABG. The CRPS values are presented relative to (divided by) those from ABG. The 5 estimators (ABG, EW(B), NP(B), NP(freq), NP(B), and ABG Kernel) are defined in Section 3. NP(BM) uses the nonparametric Algorithm 1 and estimates a Bayesian QR with the Minnesota prior of Carriero, Clark, and Marcellino (2022).

unimodality lost by ABG. In turn, they suggest that multimodalities, rather than deviations from symmetry, are the primary *economic* feature of GDP density forecasts that should be emphasized, particularly when conditioning on financial conditions. But, as also emphasized by Ganics, Rossi, and Sekhposyan (2023) in their analysis of the density forecasts from the SPF, periods when multimodalities emerge tend to be rare and short-lived. This means that accommodating them does not make a big difference when evaluating *the average* statistical performance of the models. But it affects the economic narrative.

5 Conclusion

This paper reconsiders how to construct density forecasts from quantile regressions. While quantile regression methods are finding increasing application in macroeconomics and finance, as one means of accommodating nonlinear relationships, the specific issue of how to construct density forecasts from quantile regressions has received less attention. In the macroeconomic and finance literature, following ABG, it has become popular to assume a specific parametric form when matching the quantile forecasts to a density forecast. We reconsider nonparametric approaches to constructing predictive densities from quantile regressions, estimated either by frequentist or by Bayesian methods, and compare these with the parametric approach. We suggest a simple simulation-based algorithm. Unlike the parametric approach of ABG, we

find that it can flexibly accommodate various distributional shapes.

In an application revisiting ABG, our proposed nonparametric approach corroborates the finding of Adrian, Boyarchenko, and Giannone (2021) that the conditional density of GDP growth in the US can exhibit multimodality, especially during recessionary periods. These multimodalities in GDP growth are found to be increasingly prominent when the density forecasts, as suggested by ABG, are conditioned on financial conditions. But while Adrian, Boyarchenko, and Giannone (2021) are forced to move away from the QR framework of ABG to document this novel empirical fact, we show that this finding is indeed shared by QR-based density forecasts - as long as we let the "data speak." However, we need to let the "data speak" not just when we model GDP growth with respect to financial conditions, via the first-step quantile regressions, but also when we subsequently construct the forecast densities from the quantile forecasts.

Accordingly, this paper supports the addition of QR methods to the toolkit of the macro modeler. But it suggests that, when constructing density forecasts from quantile forecasts, it is better to respect the nonparametric flavor of QR by also using non- (or semi-) parametric methods to construct the density. Importantly, these methods provide similarly accurate, even improved (on some metrics) out-of-sample, density forecasts for US GDP growth. The methods are also operational irrespective of whether the first-step QRs are estimated via frequentist or Bayesian methods. Relative to ABG and their assumption that the forecast density is skewed-t, our nonparametric approach unmasks deviations from unimodality in GDP growth forecast densities when conditioned on financial conditions. The evolution of multimodalities, rather than asymmetries, then becomes the central macroeconomic narrative for the conditional predictive distribution of GDP growth. Following Adrian, Boyarchenko, and Giannone (2021), this calls for structural macroeconomic models able to accommodate these new empirical features, such as, for example, the nonlinear dynamic stochastic general equilibrium model of Rottner (2023) that allows for excessive leverage accumulation and endogenous financial crises. Ultimately, as a nonparametric (reduced-form) modeling tool, QRs cannot discriminate between alternative structural explanations for the drivers of movements in the GDP growth density. But QRs can provide, especially when, as we suggest in this paper, the density is fitted to the quantile forecasts nonparametrically, a flexible way of modeling and forecasting this density.

References

Aastveit, K. A., J. Mitchell, F. Ravazzolo, and H. K. van Dijk (2019). "The Evolution of Forecast Density Combinations in Economics". *Oxford Research Encyclopedia of Economics and Finance*. Oxford University Press. doi. 10.1093/acrefore/9780190625979.013.381.

Adrian, T., N. Boyarchenko, and D. Giannone (2019). "Vulnerable Growth". *American Economic Review,* 109, 1263–1289. doi. 10.1257/aer.20161923.

— (2021). "Multimodality in Macrofinancial Dynamics". *International Economic Review,* 62, 861–886. doi. 10.1111/iere.12501.

Amburgey, A. and M. W. McCracken (2023). "On the Real-Time Predictive Content of Financial Condition Indices for Growth". *Journal of Applied Econometrics,* 38, 137–163. doi. 10.1002/jae.2943.

Azzalini, A. and A. Capitanio (2003). "Distributions Generated by Perturbation of Symmetry with Emphasis on a Multivariate Skew t-Distribution". *Journal of the Royal Statistical Society: Series B,* 65, 367–389. doi. 10.1111/1467-9868.00391.

Benati, L. and P. Surico (2009). "VAR Analysis and the Great Moderation". *American Economic Review,* 99, 1636–52. doi. 10.1257/aer.99.4.1636.

Brownlees, C. and A. B. Souza (2021). "Backtesting Global Growth-at-Risk". *Journal of Monetary Economics,* 118, 312–330. doi. 10.1016/j.jmoneco.2020.11.003.

Caldara, D., D. Cascaldi-Garcia, P. Cuba-Borda, and F. Loria (2021). "Understanding Growth-at-Risk: A Markov Switching Approach". mimeo, Federal Reserve Board.

Carriero, A., T. E. Clark, and M. Marcellino (2022). "Nowcasting Tail Risks to Economic Activity at a Weekly Frequency". *Journal of Applied Econometrics,* 37, 843–866. doi. 10.1002/jae.2903.

— (2023). "Capturing Macroeconomic Tail Risks with Bayesian Vector Autoregressions". *Journal of Money, Credit and Banking,* Forthcoming. doi. 10.26509/frbc-wp-202002r.

Chen, L., J. J. Dolado, and J. Gonzalo (2021). "Quantile Factor Models". *Econometrica,* 89, 875–910. doi. 10.3982/ecta15746.

Cheng, M.-Y. and P. Hall (1998). "Calibrating the Excess Mass and Dip Tests of Modality". *Journal of the Royal Statistical Society: Series B (Statistical Methodology),* 60, 579–589. doi. 10.1111/1467-9868.00141.

Chernozhukov, V. (2005). "Extremal Quantile Regression". *The Annals of Statistics,* 33, 806–839. doi. 10.1214/009053604000001165.

Chernozhukov, V., I. Fernández-Val, and A. Galichon (2010). "Quantile and Probability Curves Without Crossing". *Econometrica,* 78, 1093–1125. doi. 10.3982/ecta7880.

Delle Monache, D., A. De Polis, and I. Petrella (2023). "Modeling and Forecasting Macroeconomic Downside Risk". *Journal of Business and Economic Statistics,* Forthcoming. doi. 10.1080/07350015.2023.2277171.

Diebold, F. X., T. A. Gunther, and A. S. Tay (1998). "Evaluating Density Forecasts with Application to Financial Risk Management". *International Economic Review,* 39, 863–883. doi. 10.2307/2527342.

Fernandes, M., E. Guerre, and E. Horta (2021). "Smoothing Quantile Regressions". *Journal of Business and Economic Statistics,* 39, 338–357. doi. 10.1080/07350015.2019.1660177.

Ferrara, L., M. Mogliani, and J.-G. Sahuc (2022). "High-Frequency Monitoring of Growth at Risk". *International Journal of Forecasting,* 38, 582–595. doi. 10.1016/j.ijforecast.2021.06.010.

Figueres, J. M. and M. Jarocinski (2020). "Vulnerable Growth in the Euro Area: Measuring the Financial Conditions". *Economics Letters,* 191. doi. 10.1016/j.econlet.2020.109126.

Gaglianone, W. P. and L. R. Lima (2012). "Constructing Density Forecasts from Quantile Regressions". *Journal of Money, Credit and Banking,* 44, 1589–1607. doi. 10.1111/j.1538-4616.2012.00545.x.

— (2014). "Constructing Optimal Density Forecasts From Point Forecast Combinations". *Journal of Applied Econometrics,* 29, 736–757. doi. 10.1002/jae.2352.

Ganics, G., B. Rossi, and T. Sekhposyan (2023). "From Fixed-event to Fixed-horizon Density Forecasts: Obtaining Measures of Multi-horizon Uncertainty from Survey Density Forecasts". *Journal of Money, Credit and Banking,* Forthcoming.

Ghysels, E., L. Iania, and J. Striaukas (2018). *Quantile-based Inflation Risk Models.* Working Paper Research 349. National Bank of Belgium.

Giacomini, R. and H. White (2006). "Tests of Conditional Predictive Ability". *Econometrica,* 74, 1545–1578.

Giglio, S., B. Kelly, and S. Pruitt (2016). "Systemic Risk and the Macroeconomy: An Empirical Evaluation". *Journal of Financial Economics,* 119, 457–471. doi. 10.1016/j.jfineco.2016.01.010.

Gneiting, T. and A. E. Raftery (2007). "Strictly Proper Scoring Rules, Prediction, and Estimation". *Journal of the American Statistical Association,* 102, 359–378. doi. 10.1198/016214506000001437.

Gneiting, T. and R. Ranjan (2011). "Comparing Density Forecasts Using Threshold- and Quantile-Weighted Scoring Rules". *Journal of Business and Economic Statistics,* 29, 411–422. doi. 10.1198/jbes.2010.08110.

Hamilton, J. D. (1989). "A new approach to the analysis of non-stationary time series and the business cycle". *Econometrica,* 57, 357–384. doi. 10.2307/1912559.

Hartigan, J. A. and P. M. Hartigan (1985). "The Dip Test of Unimodality". *The Annals of Statistics,* 13, 70–84. doi. 10.1214/aos/1176346577.

Koenker, R. (2005). *Quantile Regression*. Cambridge University Press. doi. 10.1017/cbo9780511754098.

Koenker, R. and J. A. Machado (1999). "GMM Inference when the Number of Moment Conditions is Large". *Journal of Econometrics,* 93, 327–344. doi. 10.1016/s0304-4076(99)00014-7.

Koenker, R. and Q. Zhao (1996). "Conditional Quantile Estimation and Inference for ARCH Models". *Econometric Theory,* 12, 793–813. doi. 10.1017/s0266466600007167.

Kohns, D. and T. Szendrei (2021). "Horseshoe Prior Bayesian Quantile Regression". arXiv.org: 2006.07655.

Komunjer, I. (2013). "Quantile Prediction". Vol. 2. Handbook of Economic Forecasting. Elsevier, 961–994. doi. 10.1016/b978-0-444-62731-5.00017-8.

Korobilis, D. (2017). "Quantile Regression Forecasts of Inflation Under Model Uncertainty". *International Journal of Forecasting,* 33, 11–20. doi. 10.1016/j.ijforecast.2016.07.005.

Korobilis, D., B. Landau, A. Musso, and A. Phella (2021). *The Time-varying Evolution of Inflation Risks*. Working Paper Series 2600. European Central Bank.

Kozumi, H. and G. Kobayashi (2011). "Gibbs Sampling Methods for Bayesian Quantile Regression". *Journal of Statistical Computation and Simulation,* 81, 1565–1578. doi. 10.1080/00949655.2010.496117.

Krüger, F., S. Lerch, T. Thorarinsdottir, and T. Gneiting (2021). "Predictive Inference Based on Markov Chain Monte Carlo Output". *International Statistical Review,* 89, 274–301. doi. 10.1111/insr.12405.

Manzan, S. (2015). "Forecasting the Distribution of Economic Variables in a Data-Rich Environment". *Journal of Business and Economic Statistics,* 33, 144–164. doi. 10.1080/07350015.2014.937436.

Manzan, S. and D. Zerom (2013). "Are Macroeconomic Variables Useful for Forecasting the Distribution of U.S. Inflation?" *International Journal of Forecasting,* 29, 469–478. doi. 10.1016/j.ijforecast.2013.01.005.

Mitchell, J., A. Poon, and G.-L. Mazzi (2022). "Nowcasting Euro Area GDP Growth using Bayesian Quantile Regression". *Advances in Econometrics: Essays in Honor of M. Hashem Pesaran,* 43A, 51–72. doi. 10.1108/s0731-90532021000043a004.

Mitchell, J. and K. F. Wallis (2011). "Evaluating Density Forecasts: Forecast Combinations, Model Mixtures, Calibration and Sharpness". *Journal of Applied Econometrics,* 26, 1023–1040. doi. 10.1002/jae.1192.

Parzen, E. (1979). "Nonparametric Statistical Data Modeling". *Journal of the American Statistical Association,* 74, 105–121. doi. 10.2307/2286734.

Plagborg-Moller, M., L. Reichlin, G. Ricco, and T. Hasenzagl (2020). "When is Growth at Risk?" *Brookings Papers on Economic Activity,* 167–213.

Prasad, A., S. Elekdag, P. Jeasakul, R. Lafarguette, A. Alter, A. X. Feng, and C. Wang (2019). *Growth at Risk: Concept and Application in IMF Country Surveillance*. IMF Working Paper 2019/036. International Monetary Fund.

Reichlin, L., G. Ricco, and T. Hasenzagl (2020). *Financial Variables as Predictors of Real Growth Vulnerability*. Discussion Papers 05/2020. Deutsche Bundesbank.

Rossi, B. (2021). "Forecasting in the Presence of Instabilities: How We Know Whether Models Predict Well and How to Improve Them". *Journal of Economic Literature,* 59, 1135–90. doi. 10.1257/jel.20201479.

Rossi, B. and T. Sekhposyan (2019). "Alternative Tests for Correct Specification of Conditional Predictive Densities". *Journal of Econometrics,* 208, 638–657. doi. 10.1016/j.jeconom.2018.07.008.

Rottner, M. (2023). "Financial crises and shadow banks: A quantitative analysis". *Journal of Monetary Economics,* 139, 74–92. doi. 10.1016/j.jmoneco.2023.06.006.

Yu, K. and R. A. Moyeed (2001). "Bayesian Quantile Regression". *Statistics and Probability Letters,* 54, 437–447. doi. 10.1016/s0167-7152(01)00124-9.

Zou, H. and M. Yuan (2008). "Composite Quantile Regression and the Oracle Model Selection Theory". *The Annals of Statistics,* 36, 1108–1126. doi. 10.1214/07-aos507.

A Online Appendix for Mitchell, Poon, and Zhu: "Constructing Density Forecasts from Quantile Regressions: Multimodality in Macro-Financial Dynamics"

This appendix contains supplementary tables and figures referred to in the main paper.

A.1 Supplementary Monte Carlo results

Table A1: Average mean squared error and Kullback-Leibler (KL) distance for NP(freq) using $k = 4$ and $k = 99$

Models	**Mean**	**Variance**	**Skewness**	**Kurtosis**	**KL**
$k = 4$ **and** $T = 100$					
DGP1: Unimodal (Gaussian)	0.02	1.19	0.05	1.84	0.31
DGP2: Unimodal (Negative Skewness)	0.17	20.87	0.02	5.42	0.32
DGP3: Unimodal (Skew & High Kurtosis)	0.03	1.21	1.26	105.97	0.35
DGP4: Bimodal	0.02	0.03	0.16	0.28	0.32
DGP5: Trimodal	0.04	0.36	0.00	0.06	0.36
$k = 4$ **and** $T = 1,000$					
DGP1: Unimodal (Gaussian)	0.01	1.02	0.04	1.85	0.30
DGP2: Unimodal (Negative Skewness)	0.06	18.61	0.01	5.42	0.32
DGP3: Unimodal (Skew & High Kurtosis)	0.00	0.76	1.23	106.43	0.35
DGP4: Bimodal	0.02	0.03	0.15	0.27	0.32
DGP5: Trimodal	0.04	0.36	0.00	0.06	0.36
$k = 99$ **and** $T = 100$					
DGP1: Unimodal (Gaussian)	0.01	0.02	0.07	0.35	0.03
DGP2: Unimodal (Negative Skewness)	0.05	0.59	0.39	18.53	0.04
DGP3: Unimodal (Skew & High Kurtosis)	0.01	0.16	1.16	61.56	0.04
DGP4: Bimodal	0.00	0.00	0.01	0.02	0.03
DGP5: Trimodal	0.00	0.00	0.01	0.02	0.05
$k = 99$ **and** $T = 1,000$					
DGP1: Unimodal (Gaussian)	0.00	0.00	0.01	0.06	0.00
DGP2: Unimodal (Negative Skewness)	0.00	0.07	0.02	0.45	0.00
DGP3: Unimodal (Skew & High Kurtosis)	0.00	0.02	0.37	59.98	0.00
DGP4: Bimodal	0.00	0.00	0.00	0.00	0.01
DGP5: Trimodal	0.00	0.00	0.00	0.00	0.03

Table A2: Rejection rates (across 1,000 replications) of unimodality at 95% using the calibrated Hartigans' test

DGP	$T = 25$	$T = 50$	$T = 250$	$T = 1,000$	$T = 10,000$
			$k = 4$		
Gaussian	28.70%	30.00%	23.30%	15.20%	2.00%
Negative Skewness	18.00%	16.60%	5.30%	1.00%	0.00%
Skew & High Kurtosis	14.00%	9.70%	0.20%	0.00%	0.00%
Bimodal	94.50%	98.70%	100.00%	100.00%	100.00%
Trimodal	16.80%	8.50%	0.20%	0.00%	0.00%
			$k = 9$		
Gaussian	27.80%	13.00%	0.00%	0.00%	0.00%
Negative Skewness	21.30%	8.30%	0.00%	0.00%	0.00%
Skew & High Kurtosis	20.50%	8.00%	0.10%	0.00%	0.00%
Bimodal	93.30%	96.60%	99.90%	100.00%	100.00%
Trimodal	71.50%	18.80%	0.90%	0.00%	0.00%
			$k = 19$		
Gaussian	34.20%	11.70%	0.00%	0.00%	0.00%
Negative Skewness	31.80%	9.50%	0.00%	0.00%	0.00%
Skew & High Kurtosis	30.10%	7.90%	0.00%	0.00%	0.00%
Bimodal	91.30%	86.30%	94.20%	99.50%	100.00%
Trimodal	95.60%	94.90%	97.40%	99.90%	100.00%
			$k = 99$		
Gaussian	65.10%	31.70%	0.00%	0.00%	0.00%
Negative Skewness	62.60%	28.50%	0.00%	0.00%	0.00%
Skew & High Kurtosis	59.20%	20.30%	0.00%	0.00%	0.00%
Bimodal	96.00%	96.40%	98.70%	99.90%	100.00%
Trimodal	99.10%	99.30%	99.90%	100.00%	100.00%

Table A3: Average mean squared error and Kullback-Leibler (KL) distance for EW(freq) using $k = 4$ and $k = 99$

Models	**Mean**	**Variance**	**Skewness**	**Kurtosis**	**KL**
$k = 4$ **and** $T = 100$					
DGP1: Unimodal (Gaussian)	0.02	1.05	0.05	1.85	0.28
DGP2: Unimodal (Negative Skewness)	0.12	21.86	0.02	5.55	0.27
DGP3: Unimodal (High Kurtosis)	0.02	0.98	1.26	106.16	0.28
DGP4: Bimodal	0.02	0.03	0.14	0.26	0.62
DGP5: Trimodal	0.04	0.34	0.01	0.08	0.57
$k = 4$ **and** $T = 1,000$					
DGP1: Unimodal (Gaussian)	0.01	1.06	0.04	1.85	0.30
DGP2: Unimodal (Negative Skewness)	0.06	19.49	0.01	5.45	0.29
DGP3: Unimodal (High Kurtosis)	0.00	0.74	1.24	106.44	0.28
DGP4: Bimodal	0.02	0.03	0.15	0.27	0.62
DGP5: Trimodal	0.04	0.36	0.00	0.06	0.57
$k = 99$ **and** $T = 100$					
DGP1: Unimodal (Gaussian)	0.01	0.02	0.05	0.32	0.02
DGP2: Unimodal (Negative Skewness)	0.05	0.61	0.23	5.14	0.02
DGP3: Unimodal (High Kurtosis)	0.01	0.09	0.71	52.96	0.02
DGP4: Bimodal	0.00	0.00	0.00	0.02	0.07
DGP5: Trimodal	0.00	0.00	0.01	0.02	0.28
$k = 99$ **and** $T = 1,000$					
DGP1: Unimodal (Gaussian)	0.00	0.00	0.01	0.05	0.00
DGP2: Unimodal (Negative Skewness)	0.01	0.08	0.03	0.40	0.00
DGP3: Unimodal (High Kurtosis)	0.00	0.02	0.38	61.00	0.00
DGP4: Bimodal	0.00	0.00	0.00	0.00	0.06
DGP5: Trimodal	0.00	0.00	0.00	0.00	0.28

A.2 Alternative estimators of the tails

Here we present results when, instead of the Gaussian distribution used in the main paper (see equations (14) and (15)), we assume that the generalized extreme value (EV) distribution of type 1 (also known as the Gumbel) applies in the tails of the forecast densities. In particular, we solve:

$$\exp\left\{-\exp\left\{-\frac{x_t'\beta_{\tau_1}-\mu_1}{\sigma_1}\right\}\right\}=\tau_1, \exp\left\{-\exp\left\{-\frac{x_t'\beta_{\tau_2}-\mu_1}{\sigma_1}\right\}\right\}=\tau_2$$
$$\exp\left\{-\exp\left\{-\frac{x_t'\beta_{\tau_{k-1}}-\mu_2}{\sigma_2}\right\}\right\}=\tau_{k-1}, \exp\left\{-\exp\left\{-\frac{x_t'\beta_{\tau_k}-\mu_2}{\sigma_2}\right\}\right\}=\tau_k.$$

The EV density is commonly used when undertaking inference of extremal QRs; see Chernozhukov (2005). When repeating the main empirical exercises in the main paper using EV rather the Gaussian distribution, we show here that the densities constructed assuming EV in the tails look very similar. They also have forecasting performance similar to that presented in the main paper assuming Gaussianity in the tails.

We also experiment and report results when applying the Student-t CDF in the tails, to acknowledge that fatness in the extreme tails may be helpful in some applications. This involves fitting the density beyond the extreme quantiles by numerically solving the following set of equations:

$$T_{\nu_1}(\frac{x_t'\beta_{\tau_1}-\mu_1}{\sigma_1})=\tau_1, T_{\nu_1}(\frac{x_t'\beta_{\tau_2}-\mu_1}{\sigma_1})=\tau_2, T_{\nu_1}(\frac{x_t'\beta_{\tau_3}-\mu_1}{\sigma_1})=\tau_3$$
$$T_{\nu_2}(\frac{x_t'\beta_{\tau_{k-2}}-\mu_2}{\sigma_2})=\tau_{k-2}, T_{\nu_2}(\frac{x_t'\beta_{\tau_{k-1}}-\mu_2}{\sigma_2})=\tau_{k-1}, T_{\nu_2}(\frac{x_t'\beta_{\tau_k}-\mu_2}{\sigma_2})=\tau_k,$$

where T_ν is the t-distribution with ν degrees of freedom. Our empirical results assuming a t density in the tails are a little different from those assuming either Gaussianity or EV. The t density introduces some extra "wiggles" into the extreme tails of the forecast densities.

Figure A1: CDF of the in-sample PITs for NP(freq) and NP(freq) using alternative estimators of the tails

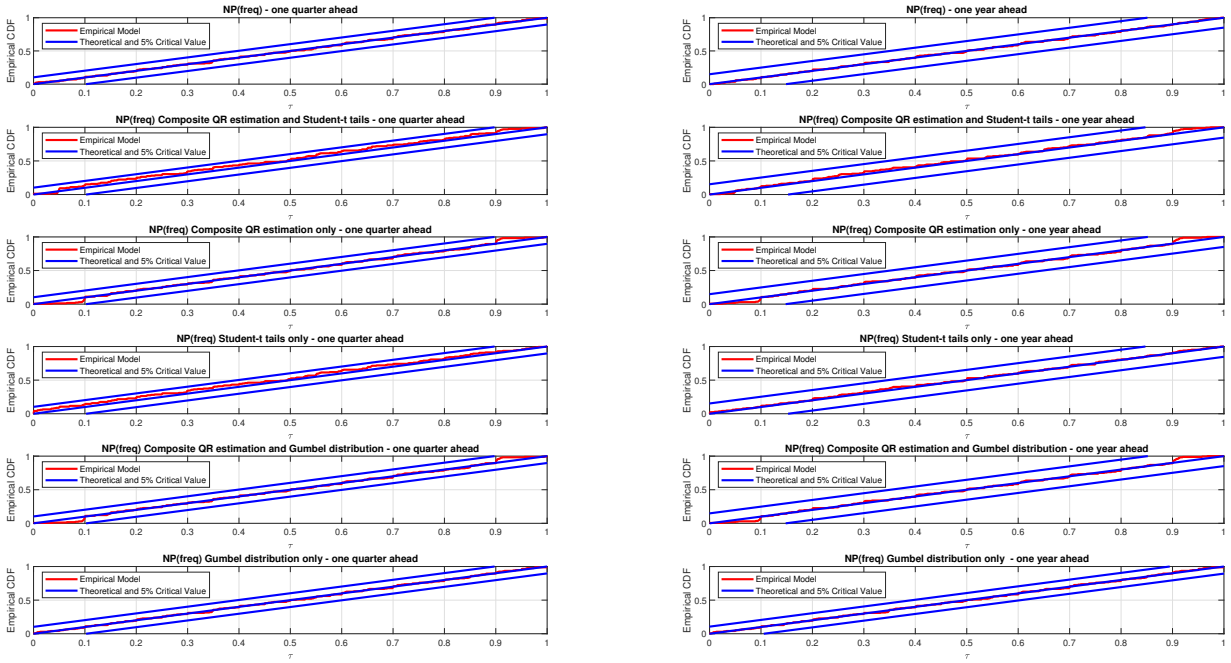

Notes: The figures show the empirical CDF of the PITs (red line), the CDF of the PITs under the null hypothesis of correct calibration (the 45-degree line), and the 5% critical value bands of the Rossi and Sekhposyan (2019) PITs test.

Figure A2: CDF of the out-of-sample PITs for NP(freq) and NP(freq) using alternative estimators of the tails

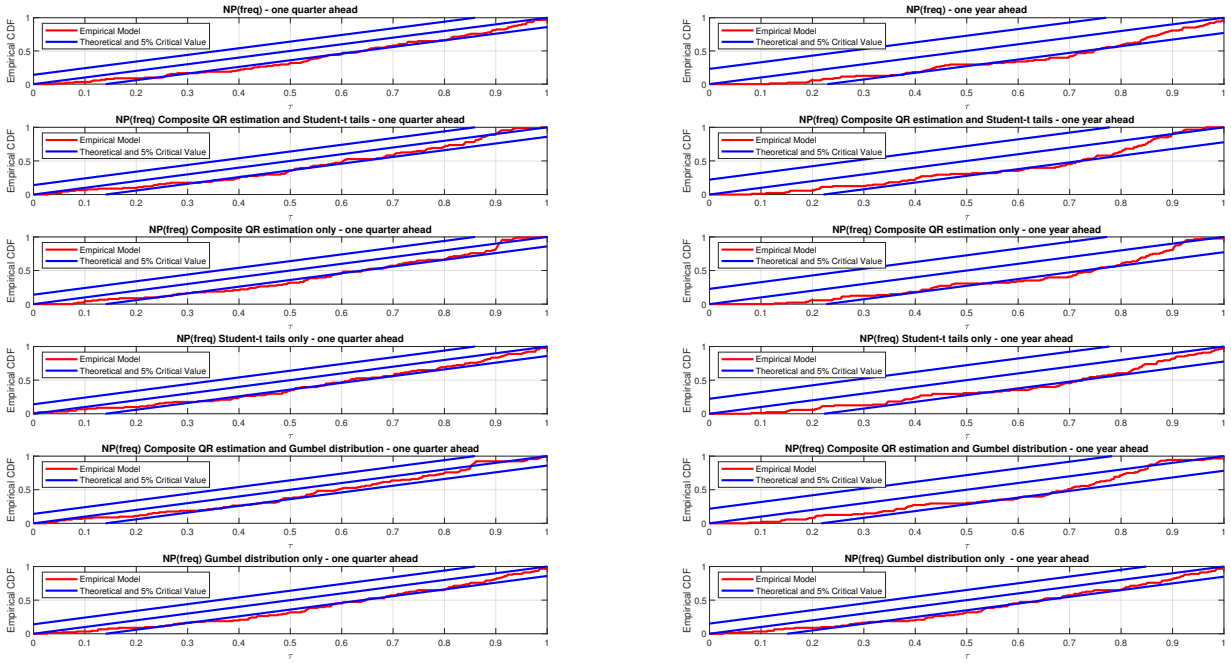

Notes: The figures show the empirical CDF of the PITs (red line), the CDF of the PITs under the null hypothesis of correct calibration (the 45-degree line), and the 5% critical value bands of the Rossi and Sekhposyan (2019) PITs test.

Table A4: Average log predictive score (LPS) and continuous ranked probability score (CRPS) for the one-quarter-ahead forecasts (out-of-sample, 1993Q1-2015Q4) and the one-year-ahead forecasts (out-of-sample, 1993Q4-2015Q4) for NP(freq) with alternative estimators of the tails

			One-quarter-ahead				
	LPS	CRPS	Left	Right	Heavy	Tails	Center
NP(freq) Composite QR estimation and Student-t tails	-3.28	1.29	0.40	0.41	0.17	0.32	0.24
NP(freq) Composite QR estimation only	-3.30	1.29	0.39	0.38	0.13	0.28	0.24
NP(freq) Student-t tails only	-3.29	1.29	0.40	0.41	0.17	0.32	0.24
NP(freq) Composite QR estimation and Gumbel distribution	-3.27	1.29	0.40	0.41	0.17	0.32	0.24
NP(freq) Gumbel distribution only	-2.44	1.26	0.40	0.41	0.17	0.32	0.24
			One-year-ahead				
NP(freq) Composite QR estimation and Student-t tails	-2.21	0.98	0.31	0.30	0.13	0.24	0.19
NP(freq) Composite QR estimation only	-2.22	0.98	0.31	0.28	0.10	0.21	0.19
NP(freq) Student-t tails only	-2.22	0.98	0.31	0.30	0.13	0.24	0.19
NP(freq) Composite QR estimation and Gumbel distribution	-2.21	0.98	0.31	0.30	0.13	0.24	0.19
NP(freq) Gumbel distribution only	-2.03	0.97	0.31	0.30	0.13	0.24	0.19

Figure A3: GDP growth density forecasts conditional on the NFCI and lagged GDP for 2008 made one-quarter-ahead (out-of-sample)

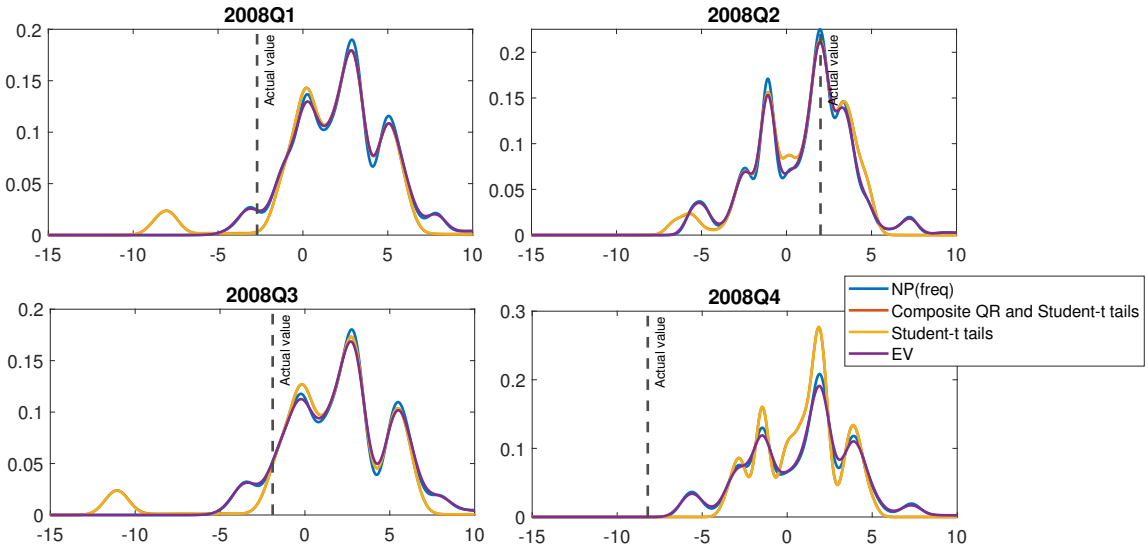

Figure A4: GDP growth density forecasts conditional on the NFCI and lagged GDP for 2008 made one-year-ahead (out-of-sample)

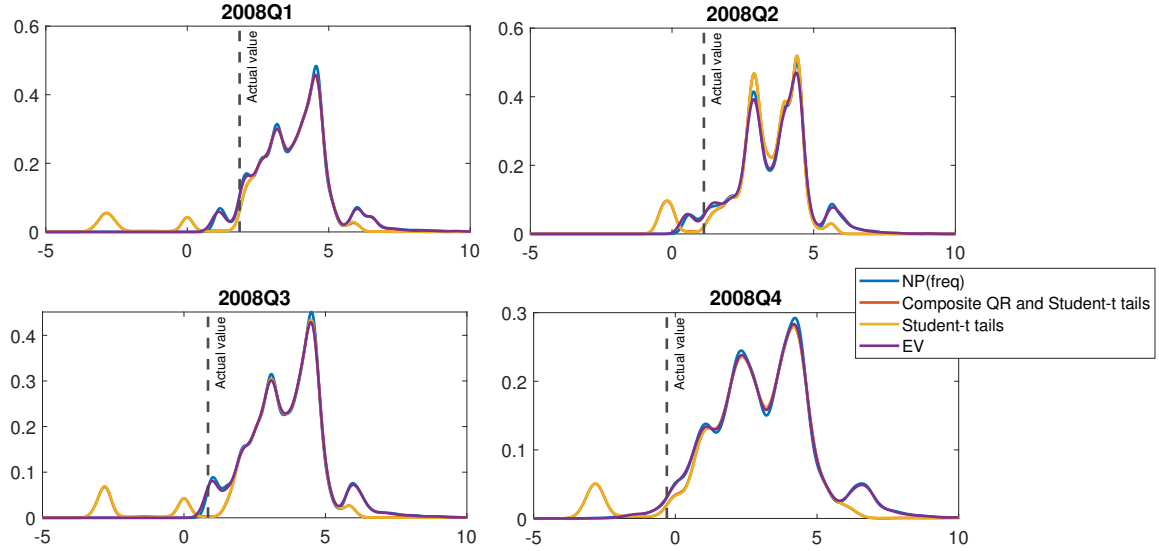

A.3 Additional tests on and analysis of the forecast densities: In-sample results

Figure A5: CDF of the in-sample PITs for ABG when $k = 19$

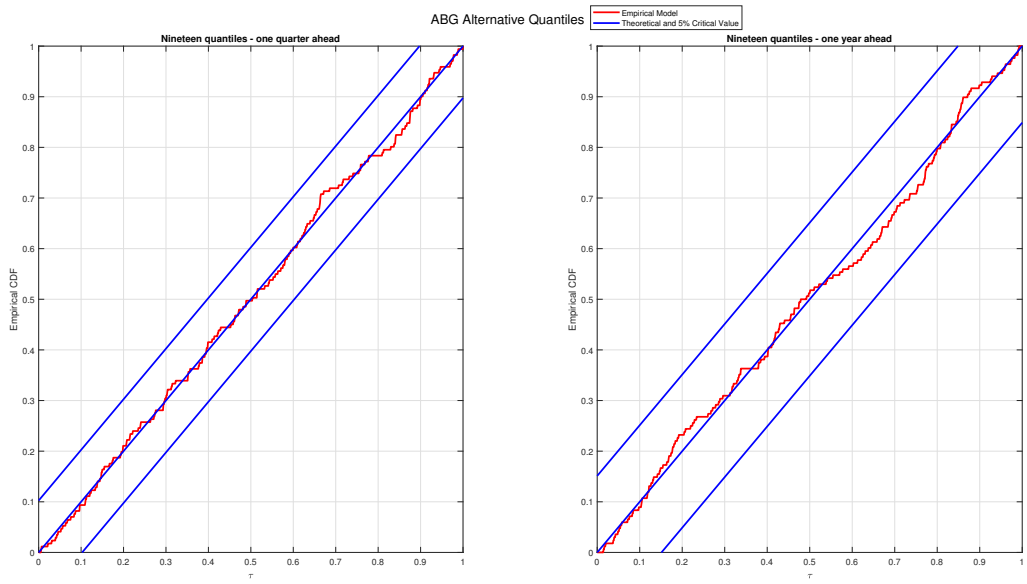

Notes: The figures show the empirical CDF of the PITs (red line), the CDF of the PITs under the null hypothesis of correct calibration (the 45-degree line), and the 5% critical value bands of the Rossi and Sekhposyan (2019) PITs test.

Figure A6: CDF of the in-sample PITs for NP(freq) when $k = 4$ and $k = 99$

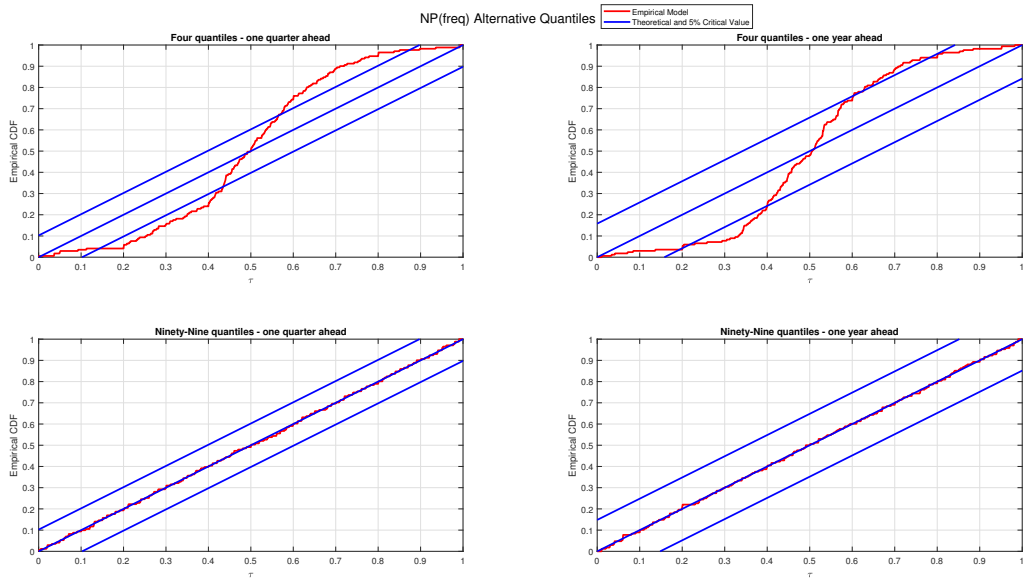

Notes: The figures show the empirical CDF of the PITs (red line), the CDF of the PITs under the null hypothesis of correct calibration (the 45-degree line), and the 5% critical value bands of the Rossi and Sekhposyan (2019) PITs test.

Figure A7: In-sample plots of the four moments of the ABG and NP(freq) forecast densities (one-quarter-ahead), when ABG's skewed-t density is simulated not truncated

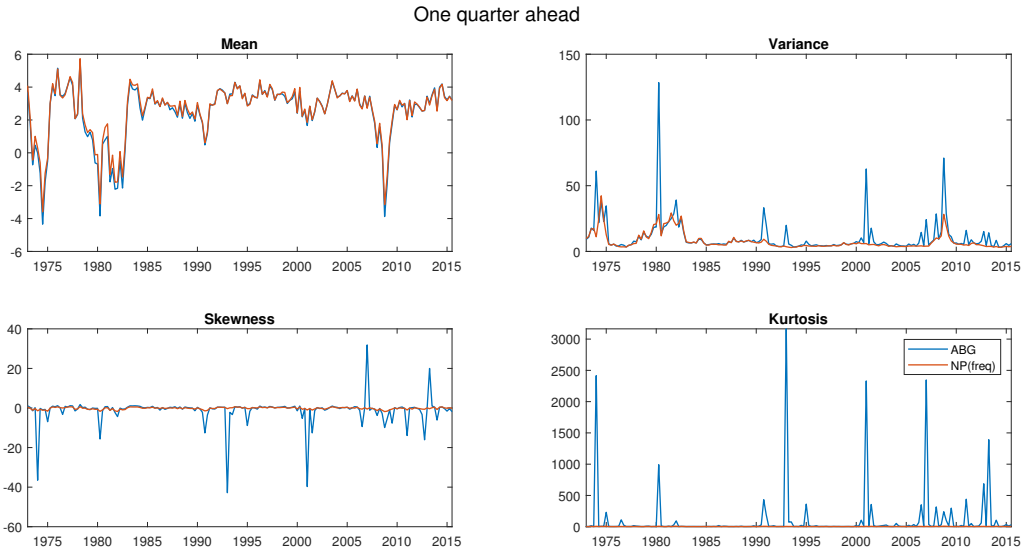

Figure A8: In-sample plots of the four moments of the ABG and NP(freq) forecast densities (one-year-ahead), when ABG's skewed-t density is simulated not truncated

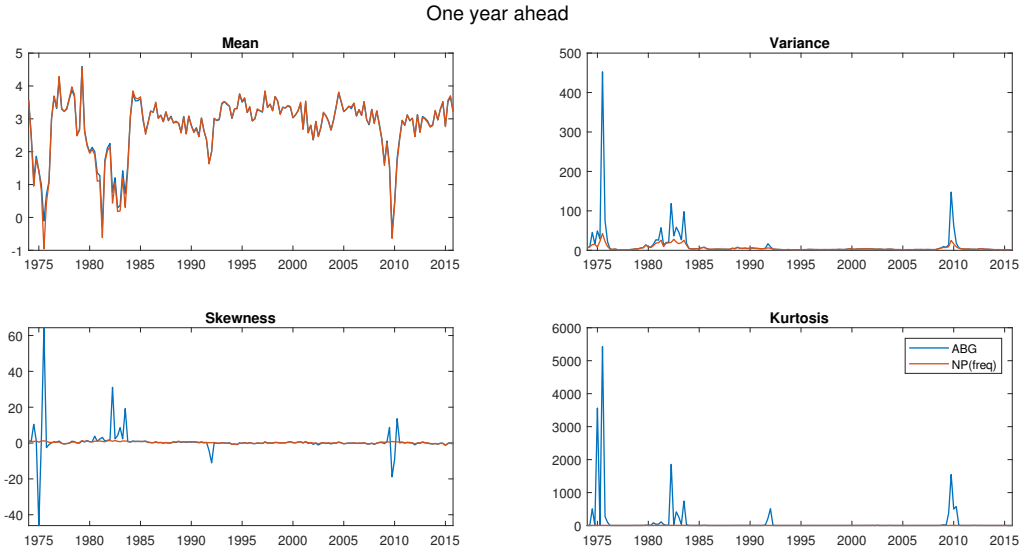

Figure A9: CDF of the in-sample PITs (one-quarter-ahead forecasts, 1993Q1-2015Q4) from the 6 density forecasts with and without the NFCI

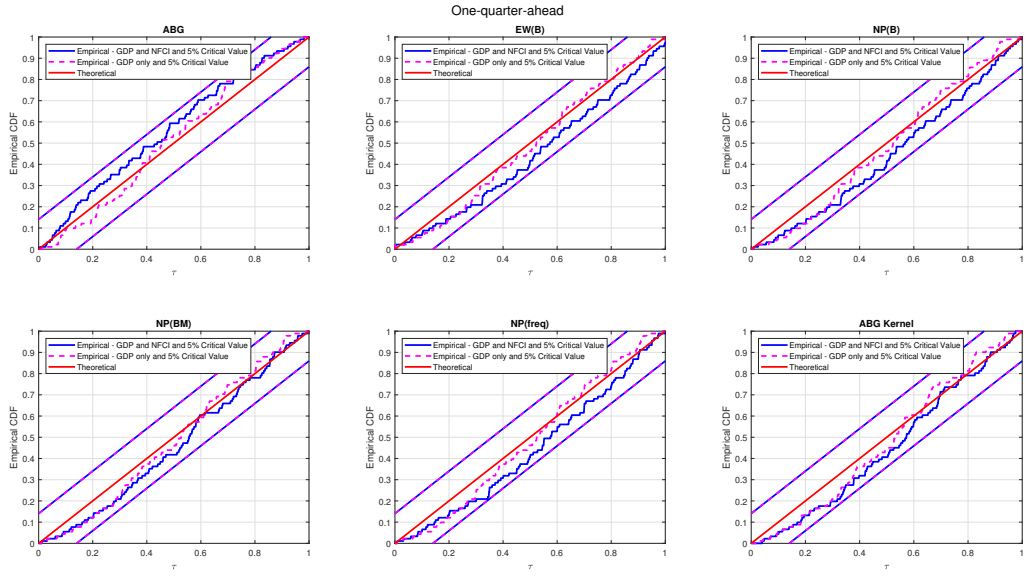

Notes: The figures show the empirical CDF of the PITs (blue line) from the QR models with the NFCI (and lagged GDP), the empirical CDF of the PITs (dashed red line) from the QR models without the NFCI, plus the CDF of the PITs under the null hypothesis of correct calibration (the 45-degree line), and the 5% critical value bands of the Rossi and Sekhposyan (2019) PITs test.

Figure A10: CDF of the in-sample PITs (one-year-ahead forecasts, 1993Q4-2015Q4) from the 6 density forecasts with and without the NFCI

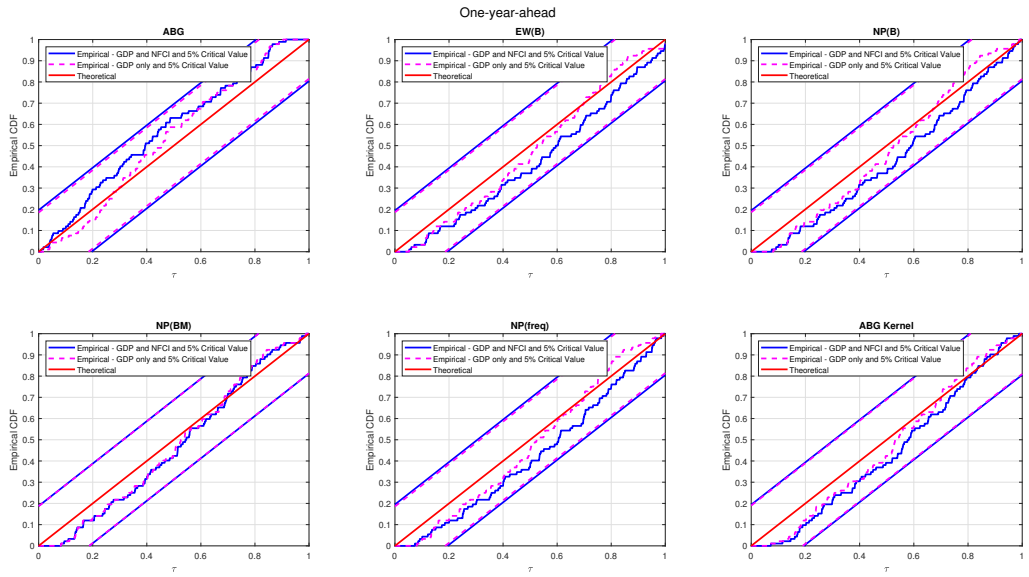

Notes: The figures show the empirical CDF of the PITs (blue line) from the QR models with the NFCI (and lagged GDP), the empirical CDF of the PITs (dashed red line) from the QR models without the NFCI, plus the CDF of the PITs under the null hypothesis of correct calibration (the 45-degree line), and the 5% critical value bands of the Rossi and Sekhposyan (2019) PITs test.

Figure A11: GDP growth density forecasts conditional on the NFCI and lagged GDP for 2005 made one-year-ahead (in-sample)

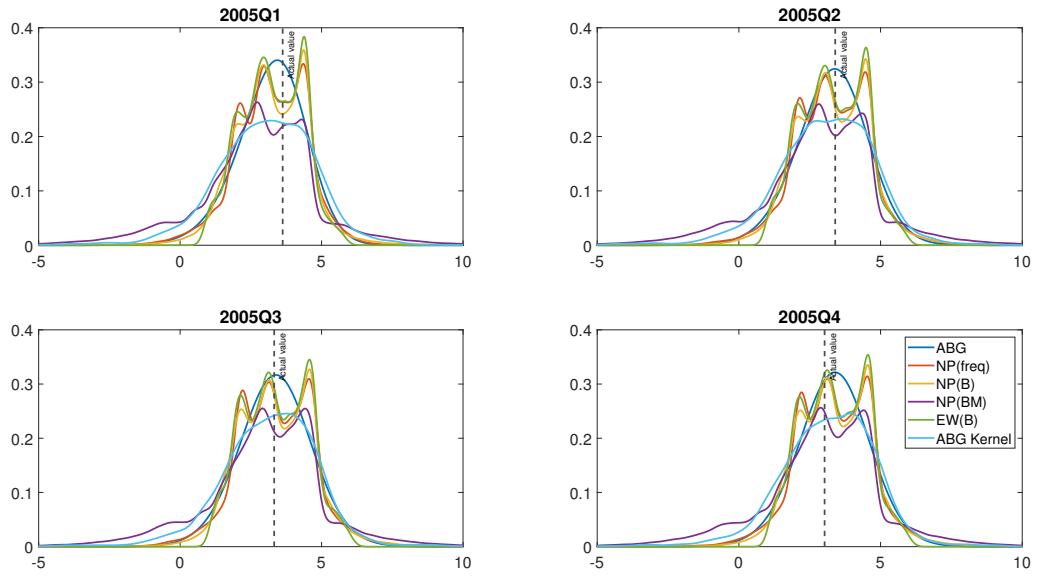

Figure A12: GDP growth density forecasts conditional on the NFCI and lagged GDP for 2008 made one-year-ahead (in-sample)

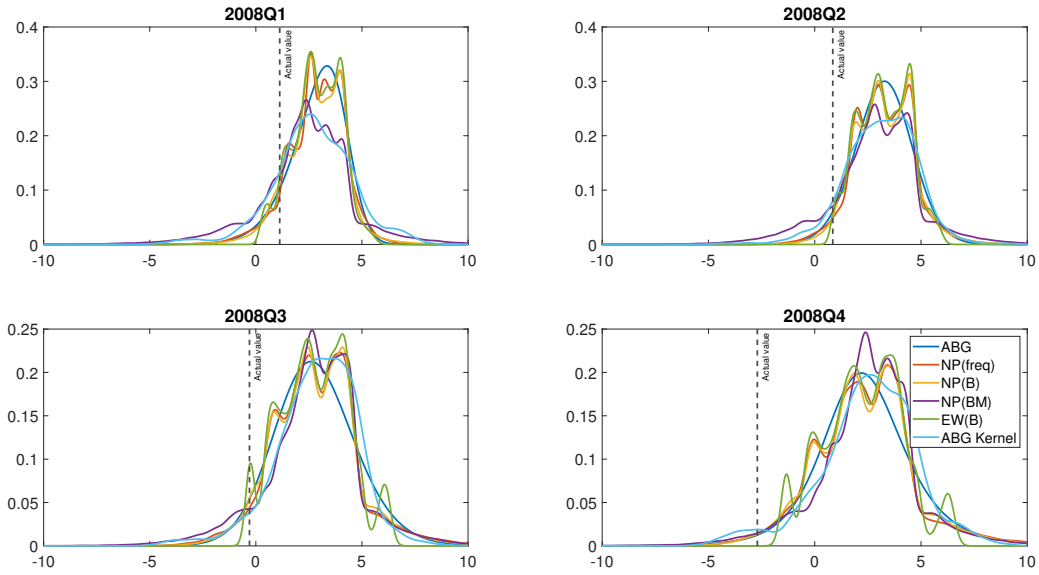

A.4 Additional tests on and analysis of the forecast densities: Out-of-sample results

Table A5: Tests on specfic regions of the distribution for the one-quarter- and one-year-ahead forecasts conditioned on both the NFCI and lagged GDP (out-of-sample, 1993Q1-2015Q4): p-values from the Rossi and Sekhposyan (2019) test on specific parts of the distribution

	Horizon	Left Tail	Left Half	Right Half	Right Tail	Center	Tails
ABG	1q	0.00	0.00	0.00	0.00	0.00	0.00
	1y	0.02	0.01	0.03	0.00	0.01	0.02
NP(BM)	1q	0.01	0.02	0.02	0.49	0.03	0.01
	1q	0.00	0.08	0.26	0.57	0.16	0.02
NP(freq)	1q	0.00	0.00	0.00	0.00	0.00	0.00
	1y	0.00	0.01	0.01	0.02	0.00	0.00

Notes: p-values from the κ_α test of Rossi and Sekhposyan (2019) when applied to the left tail $r \in [0, 0.25]$, left half $r \in [0, 0.5]$, right half $r \in [0.5, 1]$, right tail $r \in [0.75, 1]$, center $r \in [0.25, 0.20.75]$, and tails $r \in \{[0, 0.25] \cup [0.75, 1]\}$ of the forecast density, where r selects the region of the forecast distribution.

Table A6: Quantile-weighted continuous ranked probability scores (CRPS) for the one-quarter-ahead forecasts (out-of-sample, 1993Q1-2015Q4) and the one-year-ahead forecasts (out-of-sample, 1993Q4-2015Q4) that emphasize regions of interest in the forecast density for GDP growth

	One-quarter-ahead							
	With NFCI & GDP				With lagged GDP only			
	Left	Right	Tails	Center	Left	Right	Tails	Center
ABG	0.39	0.39	0.28	0.25	0.42	0.39	0.30	0.25
EW(B)	0.39	0.38	0.28	0.24	0.41	0.38	0.29	0.25
NP(B)	0.38	0.38	0.28	0.24	0.41	0.38	0.30	0.25
NP(BM)	0.38	0.38	0.28	0.24	0.41	0.38	0.30	0.25
NP(freq)	0.39	0.38	0.28	0.24	0.41	0.38	0.30	0.25
ABG Kernel	0.40	0.40	0.30	0.25	0.42	0.40	0.31	0.25
NP(PRRH)	0.36	0.37	0.27	0.23	0.36	0.36	0.27	0.23
	One-year-ahead							
ABG	0.31	0.29	0.22	0.19	0.32	0.28	0.23	0.18
EW(B)	0.31	0.28	0.21	0.19	0.32	0.26	0.22	0.18
NP(B)	0.30	0.28	0.21	0.19	0.32	0.27	0.23	0.18
NP(BM)	0.32	0.27	0.23	0.18	0.32	0.27	0.23	0.18
NP(freq)	0.31	0.28	0.21	0.19	0.32	0.27	0.23	0.18
ABG Kernel	0.32	0.30	0.23	0.20	0.33	0.28	0.23	0.19
NP(PRRH)	0.30	0.29	0.22	0.19	0.31	0.27	0.22	0.18

Notes: The weighted CRPS statistics are computed as in Gneiting and Ranjan (2011); see their Table 4 for details of the weight functions that favor the left and right tails, both tails, and the center of the forecast density.

Figure A13: GDP growth density forecasts conditional on the NFCI and lagged GDP for 2005 made one-quarter-ahead (out-of-sample)

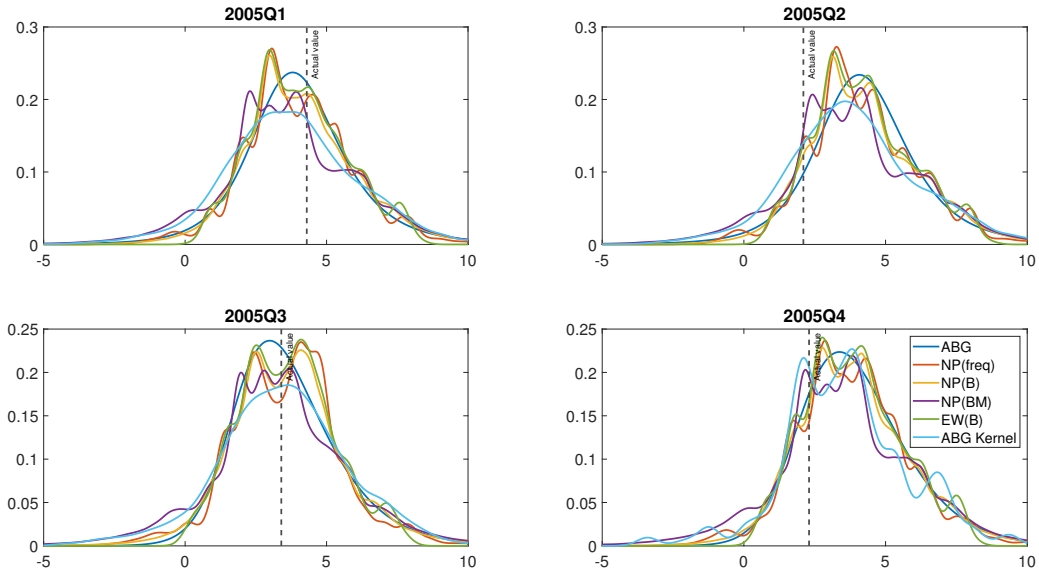

Figure A14: GDP growth density forecasts conditional on the NFCI and lagged GDP for 2008 made one-quarter-ahead (out-of-sample)

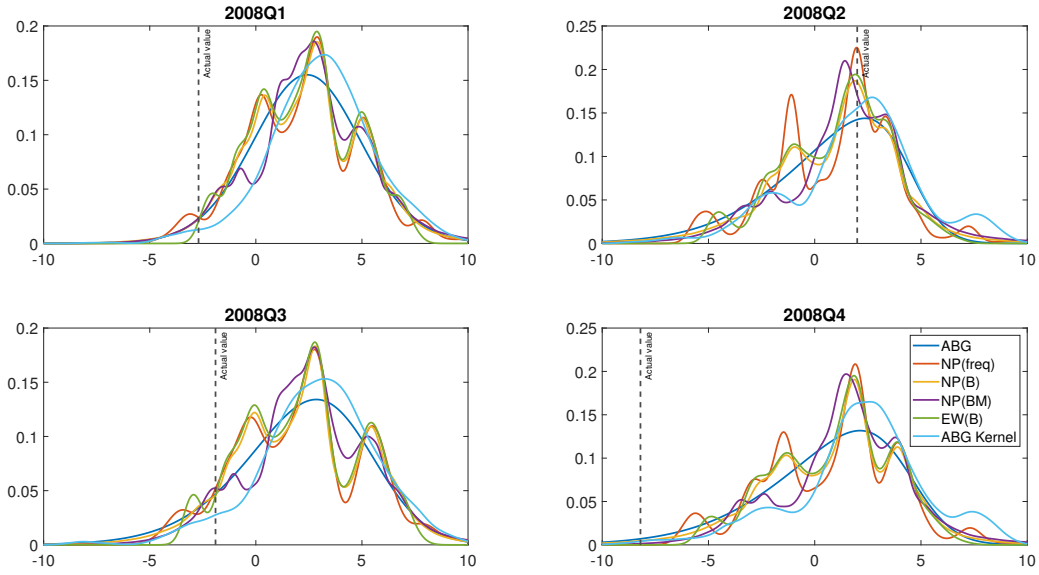

Figure A15: GDP growth density forecasts conditional on the NFCI and lagged GDP for 2005 made one-year-ahead (out-of-sample)

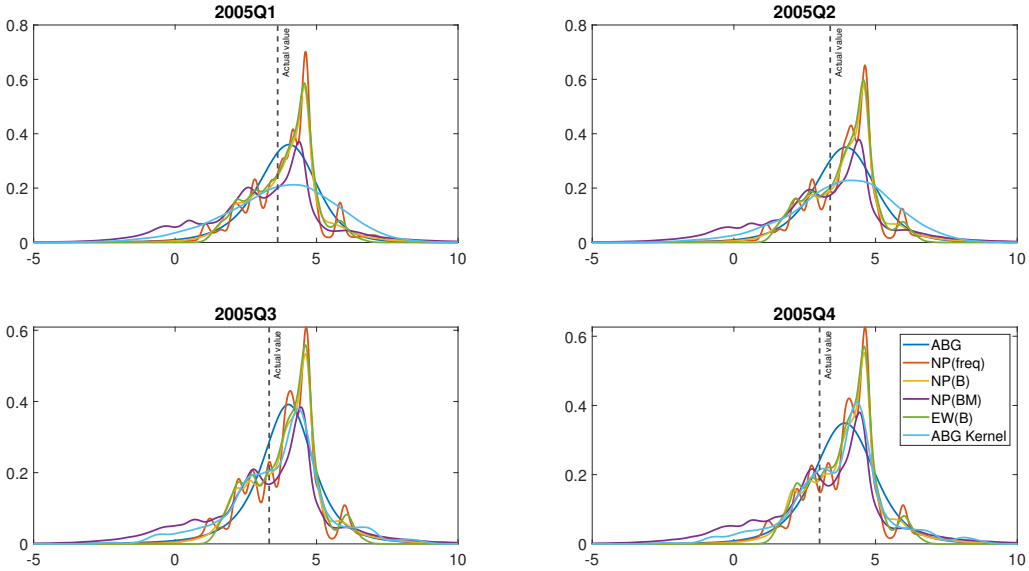

Figure A16: GDP growth density forecasts conditional on the NFCI and lagged GDP for 2008 made one-year-ahead (out-of-sample)

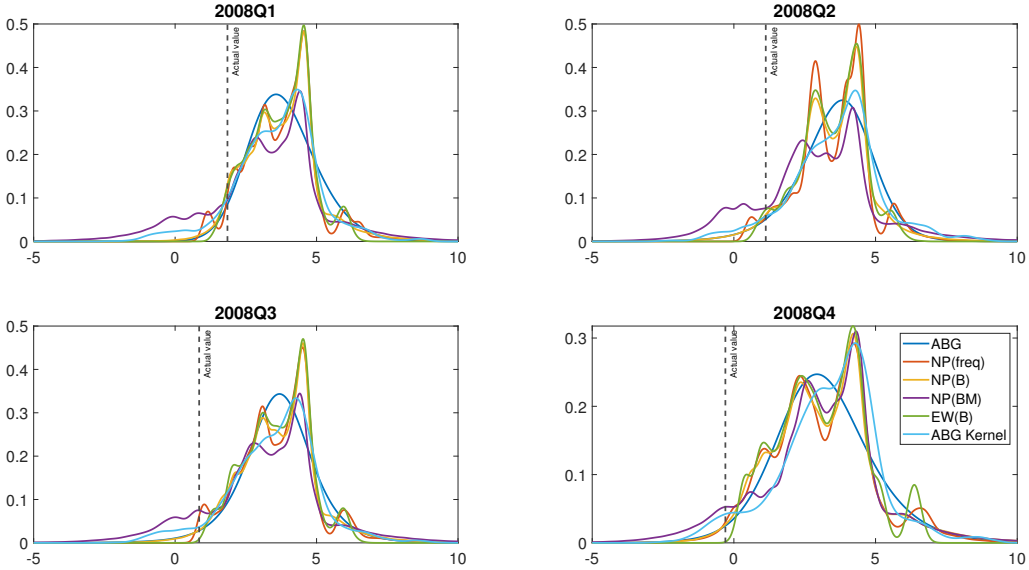

Figure A17: P-values over Time from the Calibrated Hartigans' Unimodality Test for NP(freq)

Panel A: NFCI and GDP

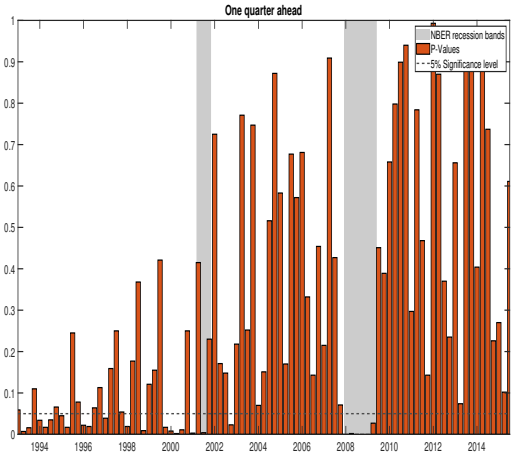

Panel B: NFCI and GDP

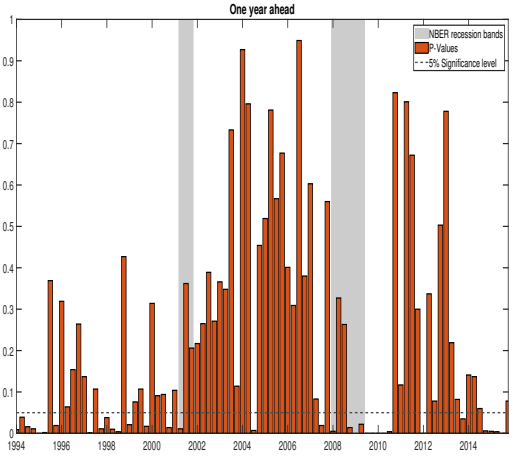

Panel C: GDP only

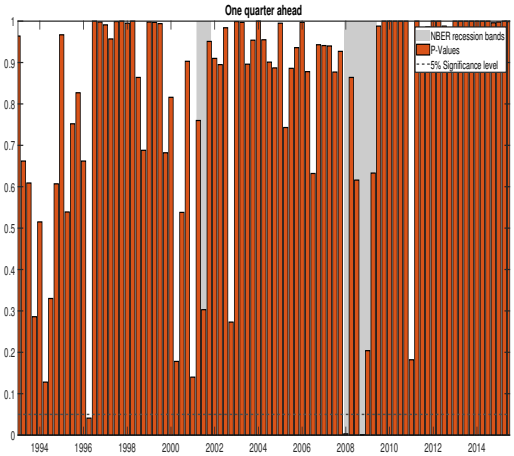

Panel D: GDP only

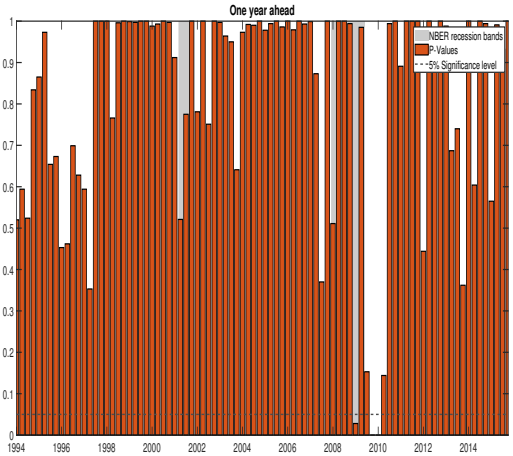

Notes: Panel A shows the p-values from the Hartigans' unimodality test (one-quarter-ahead) for the NP(freq) out-of-sample GDP growth density forecasts conditional on the NFCI and lagged GDP. Panel B shows the p-values from the Hartigans' unimodality test over time (one-year-ahead) for the NP(freq) in-sample GDP growth density forecasts conditional on the NFCI and lagged GDP. Panel C shows the p-values from the Hartigans' unimodality test over time (one-quarter-ahead) for the NP(freq) in-sample GDP growth density forecasts conditional on only lagged GDP. Panel D shows the p-values from the Hartigans' unimodality test over time (one-year-ahead) for the NP(freq) in-sample GDP growth density forecasts conditional on only lagged GDP. NBER recessionary periods are shaded gray.

Figure A18: P-values over Time from the Calibrated Hartigans' Unimodality Test for NP(PRRH)

Panel A: PRRH factors and GDP

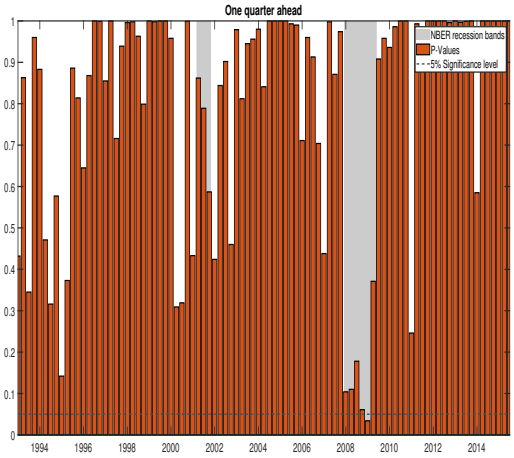

Panel B: PRRH factors and GDP

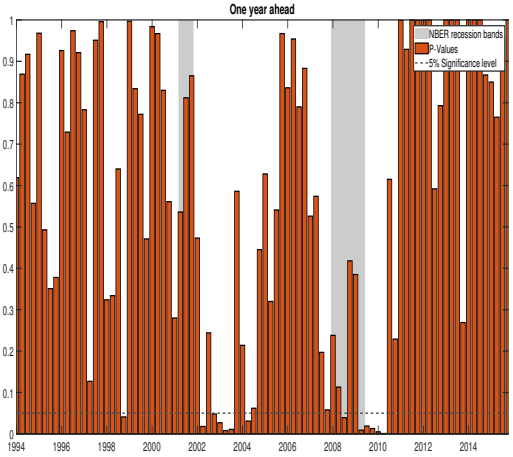

Panel C: GDP and global factor only

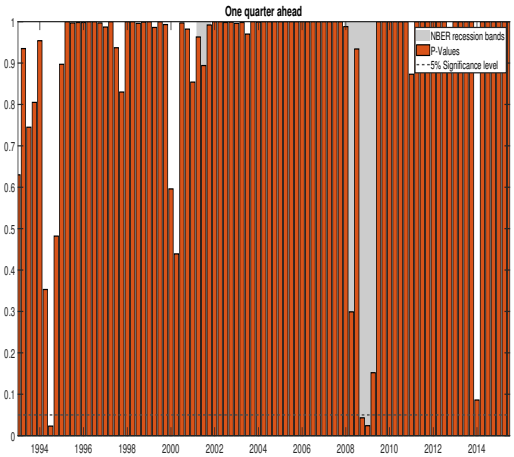

Panel D: GDP and global factor only

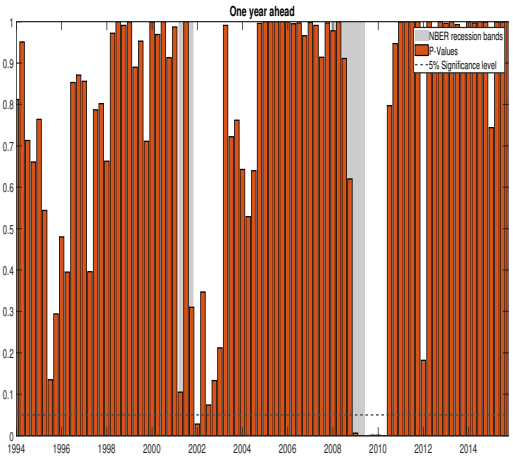

Notes: Panel A shows the p-values from the Hartigans' unimodality test (one-quarter-ahead) for the NP(PRRH) out-of-sample GDP growth density forecasts conditional on both the "global" and "financial" factors from PRRH and lagged GDP. Panel B shows the p-values from the Hartigans' unimodality test over time (one-year-ahead) for the NP(PRRH) in-sample GDP growth density forecasts conditional on both the 'global" and "financial" factors from PRRH and lagged GDP. Panel C shows the p-values from the Hartigans' unimodality test over time (one-quarter-ahead) for the NP(PRRH) in-sample GDP growth density forecasts conditional on only lagged GDP and the global factor from PRRH. Panel D shows the p-values from the Hartigans' unimodality test over time (one-year-ahead) for the NP(PRRH) in-sample GDP growth density forecasts conditional on only lagged GDP and the global factor from PRRH. NBER recessionary periods are shaded gray.

Figure A19: Out-of-sample LPS (one-quarter-ahead, 1993Q1-2015Q4)

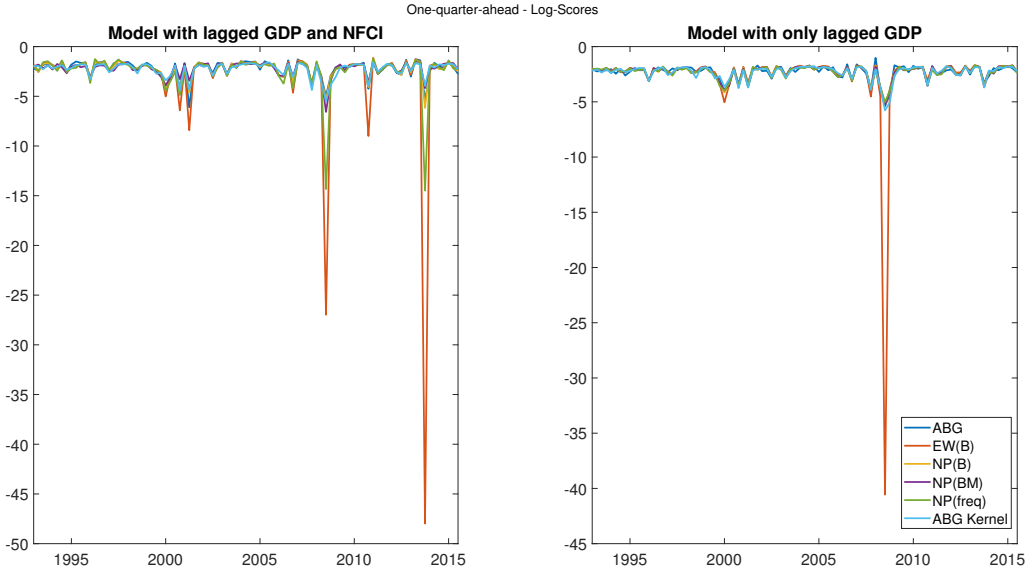

Figure A20: Out-of-sample LPS (one-year-ahead, 1993Q4-2015Q4)

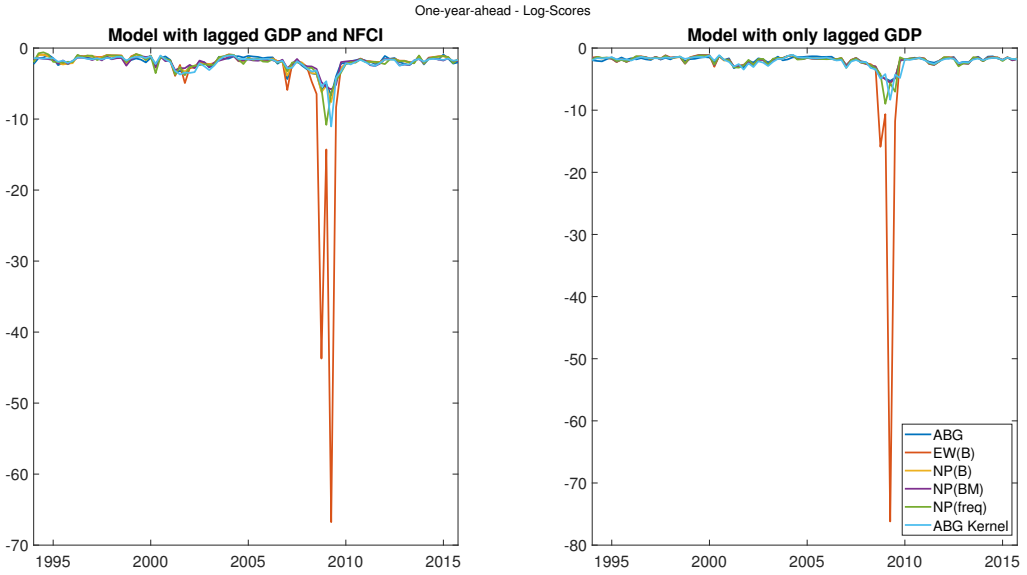

A.5 Additional results for NP(freq)

Figure A21: GDP growth density forecasts conditional on the NFCI and lagged GDP for 2005 made one-quarter-ahead (in-sample): illustrating the sensitivity of NP(freq) to k (the number of quantiles)

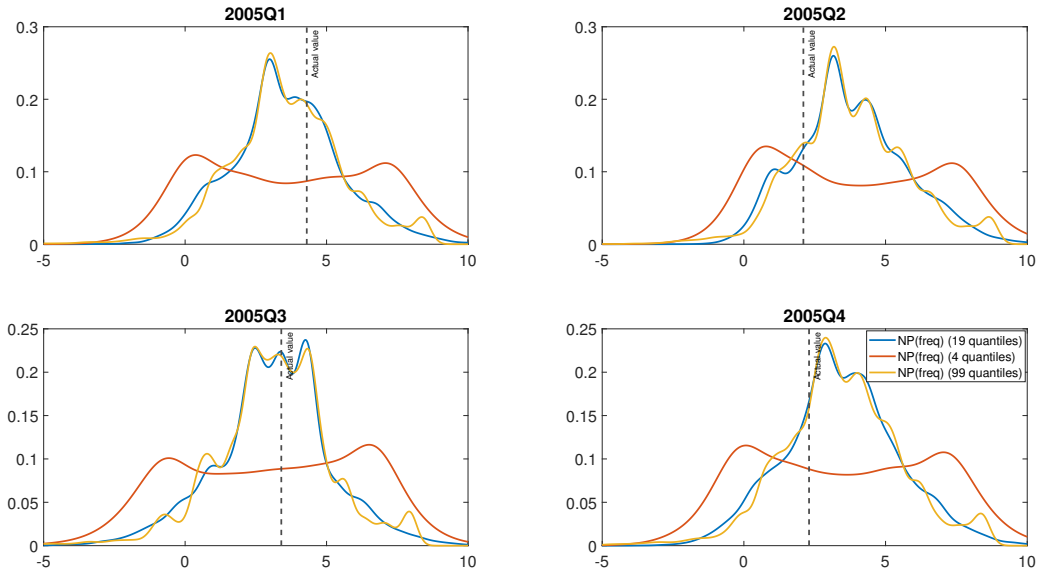

Figure A22: GDP growth density forecasts conditional on the NFCI and lagged GDP for 2008 made one-quarter-ahead (in-sample): illustrating the sensitivity of NP(freq) to k (the number of quantiles)

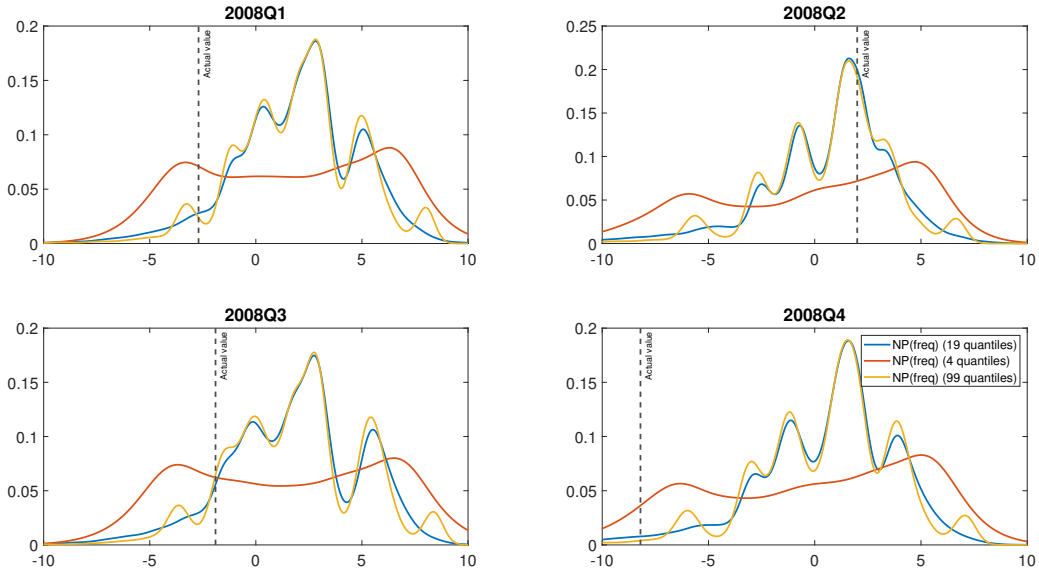

A.6 Consideration of an extended set of predictors

Here we report illustrative results when we repeat the QR analysis in the main paper, but consider an extended set of predictors for GDP growth. Specifically, we estimate QRs that use as predictors not just lagged GDP but also the global and financial factors suggested by Plagborg-Moller et al. (2020) (henceforth PRRH).

Table A7: Average log predictive score (LPS) and continuous ranked probability score (CRPS) for the one-quarter-ahead forecasts (out-of-sample, 1993Q1-2015Q4) and the one-year-ahead forecasts (out-of-sample, 1993Q4-2015Q4)

	With NFCI & GDP				With lagged GDP only			
	One-quarter-ahead		One-year-ahead		One-quarter-ahead		One-year-ahead	
	LPS	CRPS	LPS	CRPS	LPS	CRPS	LPS	CRPS
ABG	-2.24	1.27	-2.02	0.98	-2.31	1.32	-1.99	0.96
EW(B)	-0.81	0.98	-1.27	0.99	-0.36	0.97	-1.06	0.98
NP(B)	-0.01	0.98	0.02	0.99	0.00	0.98	-0.03	1.00
NP(BM)	0.01	0.98	0.01	0.98	0.00	0.98	-0.03	1.00
NP(freq)	-0.23	0.99	-0.03	0.99	-0.02	0.98	-0.09	1.00
ABG Kernel	-0.03	1.03	-0.09	1.04	-0.03	1.00	-0.11	1.03
NP(PRRH)	-0.01	0.95	0.06	0.99	0.11	0.89	-0.03	0.99

Notes: The LPS values are presented relative to (by subtraction of) the LPS from ABG. The CRPS values are presented relative to (divided by) those from ABG. The 5 estimators (ABG, EW(B), NP(B), NP(freq), NP(B), and ABG Kernel) are defined in Section 3. NP(BM) uses the nonparametric Algorithm 1 and estimates a Bayesian QR with the Minnesota prior of Carriero, Clark, and Marcellino (2022).

Figure A23: GDP growth density forecasts conditional on the NFCI and lagged GDP for 2005 made one-quarter-ahead (in-sample)

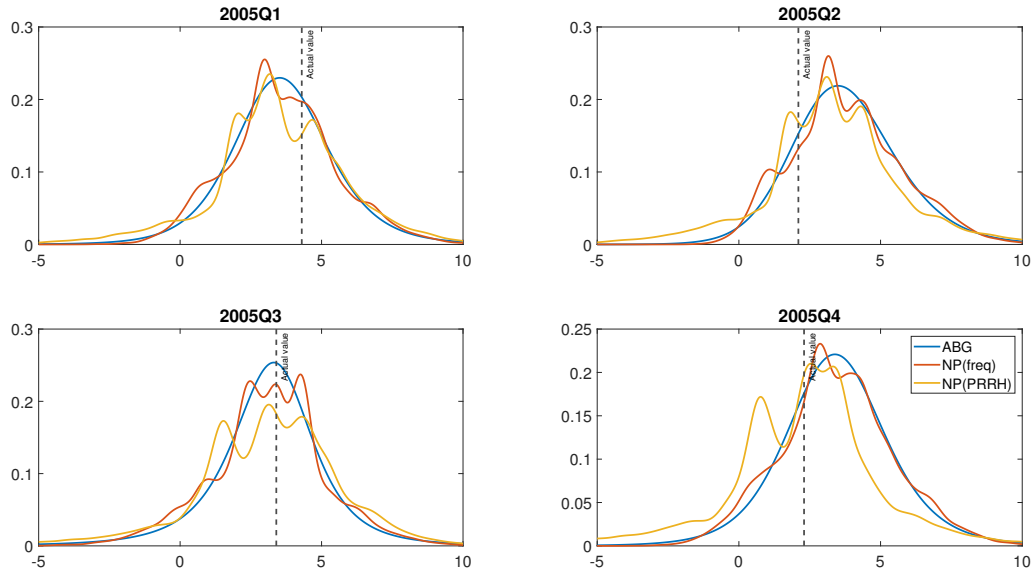

Figure A24: GDP growth density forecasts conditional on the NFCI and lagged GDP for 2008 made one-quarter-ahead (in-sample)

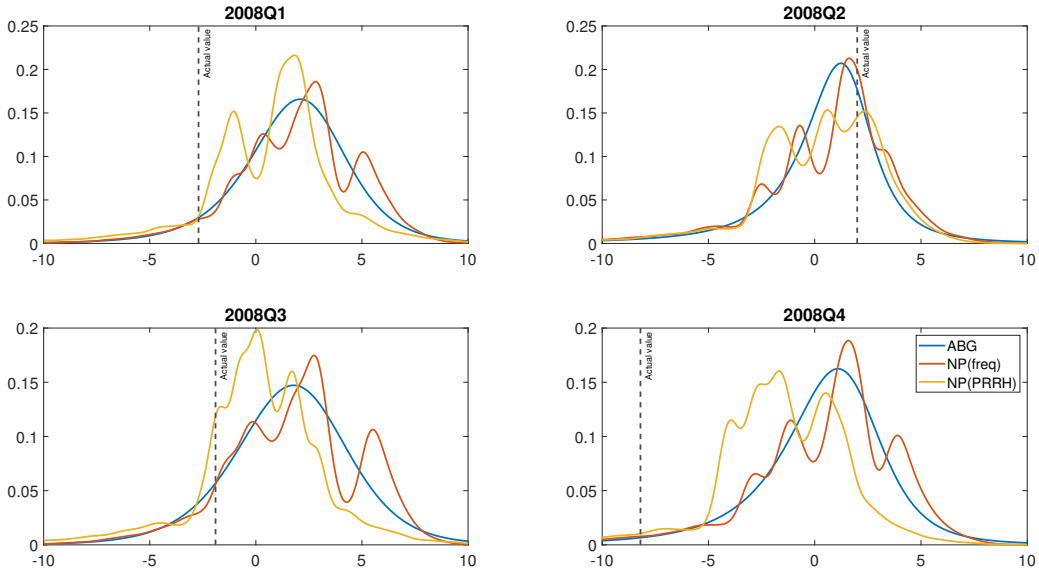

Figure A25: GDP growth density forecasts conditional on the NFCI and lagged GDP for 2005 made one-year-ahead (in-sample)

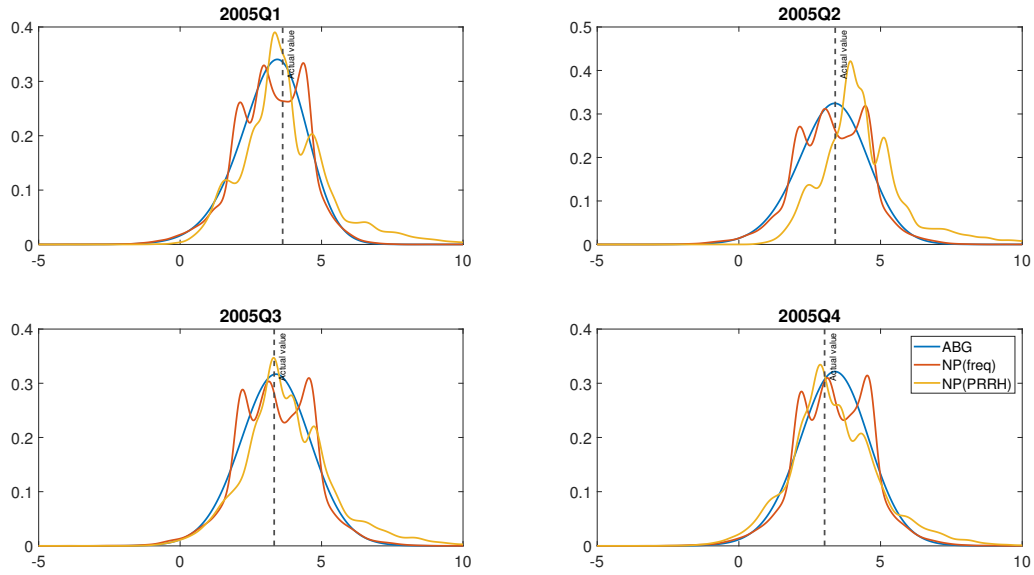

Figure A26: GDP growth density forecasts conditional on the NFCI and lagged GDP for 2008 made one-year-ahead (in-sample)

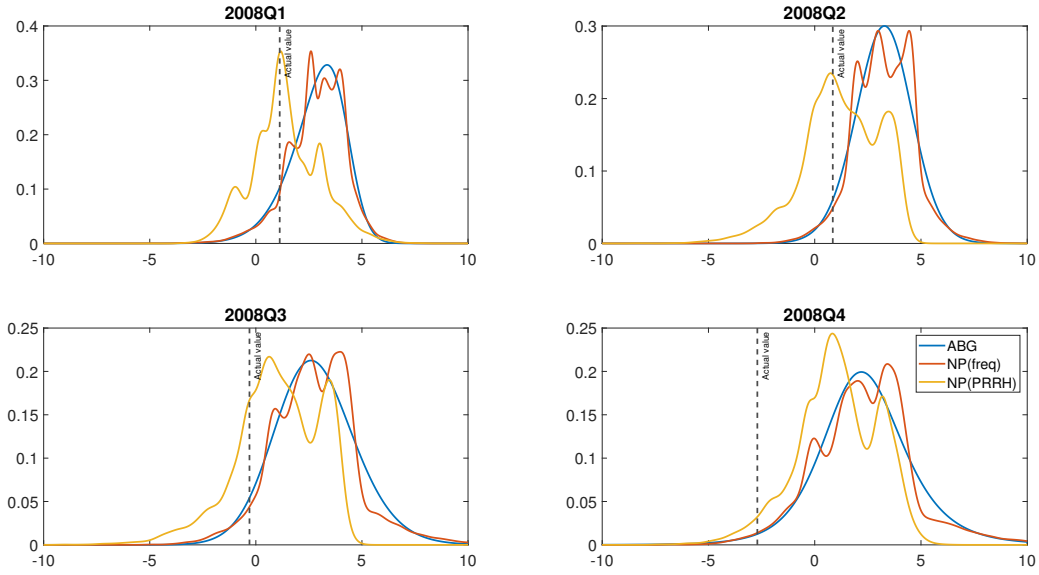

Figure A27: GDP growth density forecasts conditional on the NFCI and lagged GDP for 2005 made one-quarter-ahead (out-of-sample)

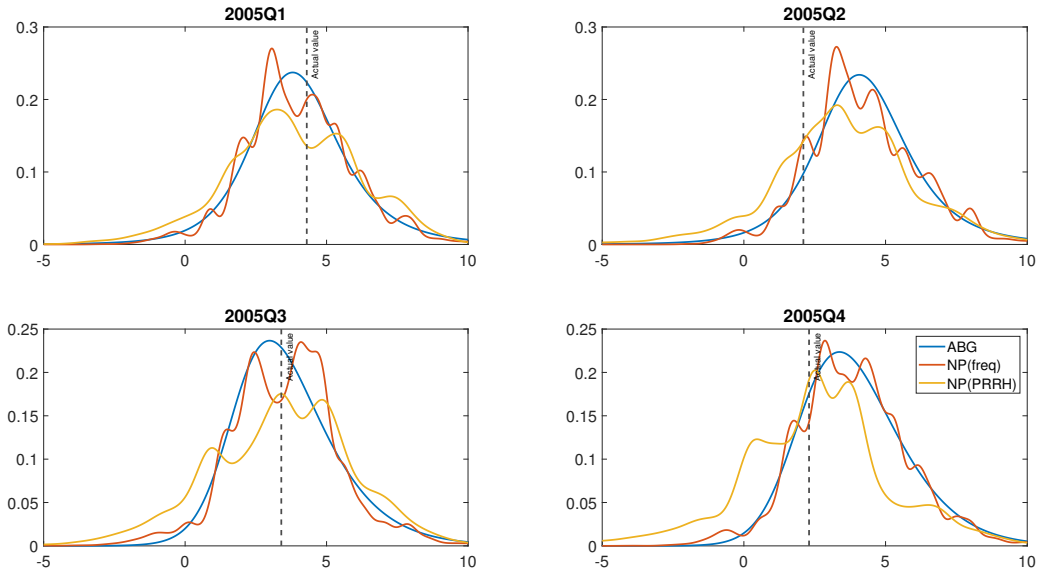

Figure A28: GDP growth density forecasts conditional on the NFCI and lagged GDP for 2008 made one-quarter-ahead (out-of-sample)

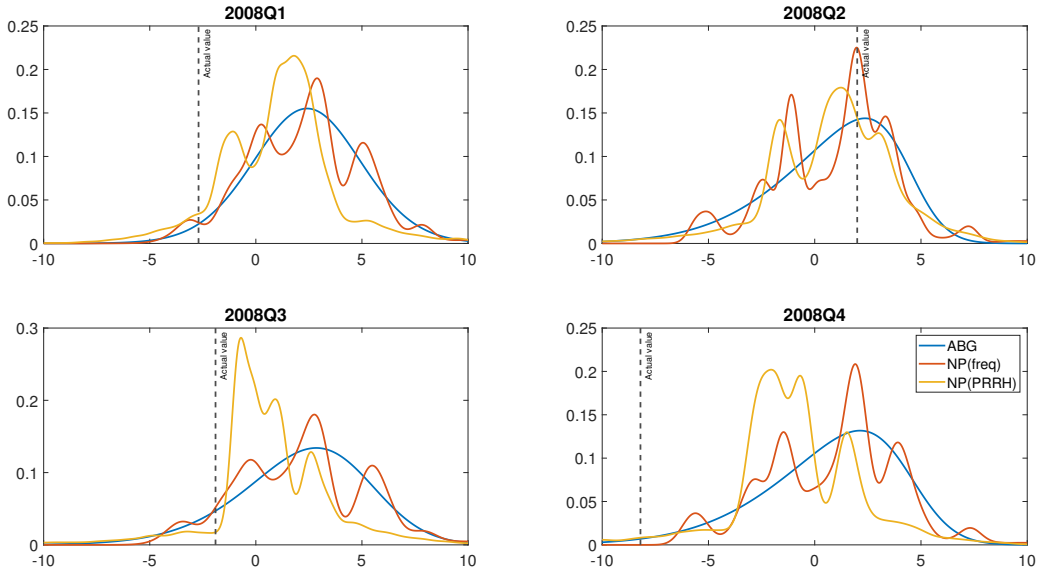

Figure A29: GDP growth density forecasts conditional on the NFCI and lagged GDP for 2005 made one-year-ahead (out-of-sample)

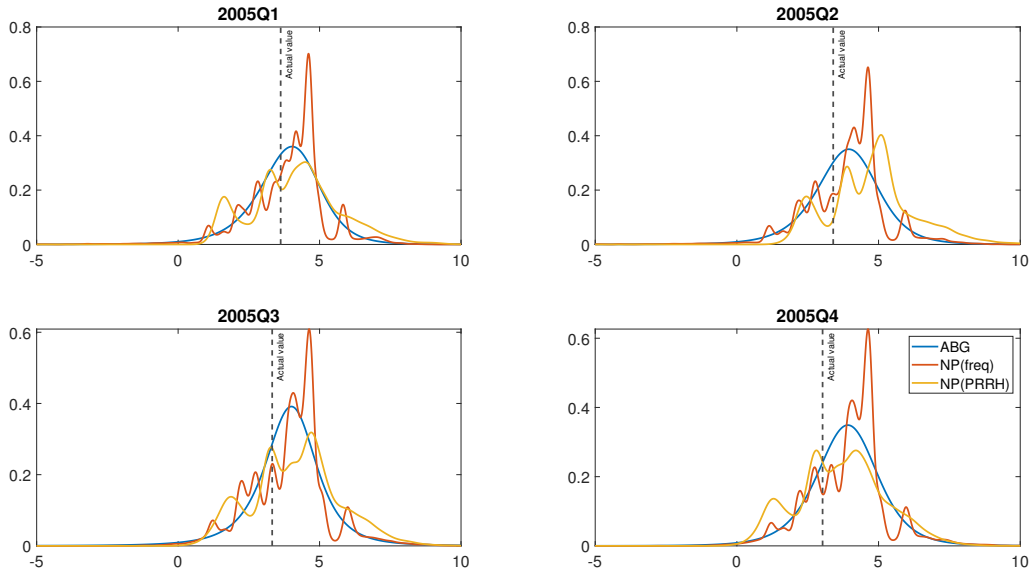

Figure A30: GDP growth density forecasts conditional on NFCI and lagged GDP for 2008 made one-year-ahead (out-of-sample)

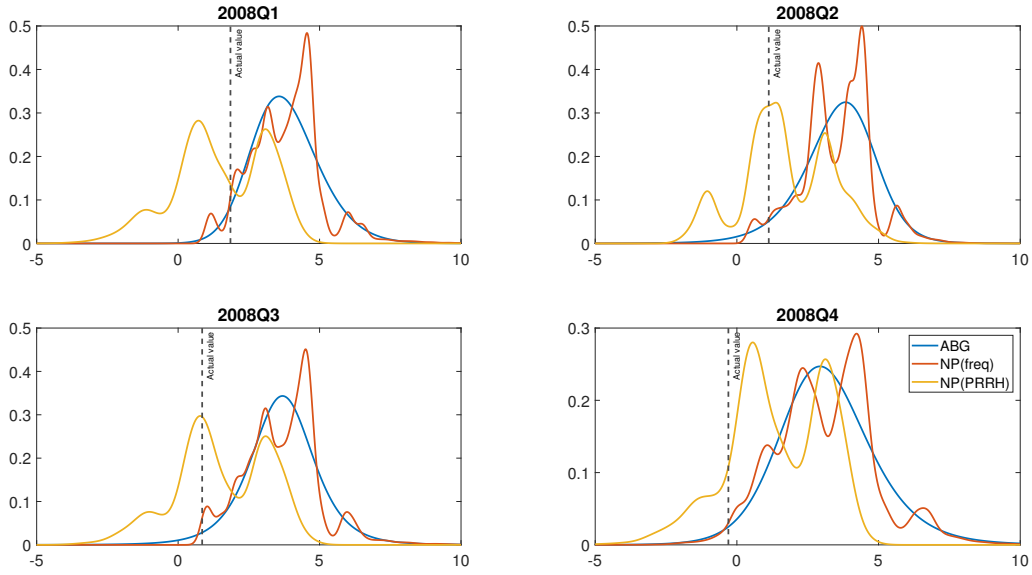

Figure A31: CDF of the in-sample PITs from ABG, NP(freq), and NP(PRRH)

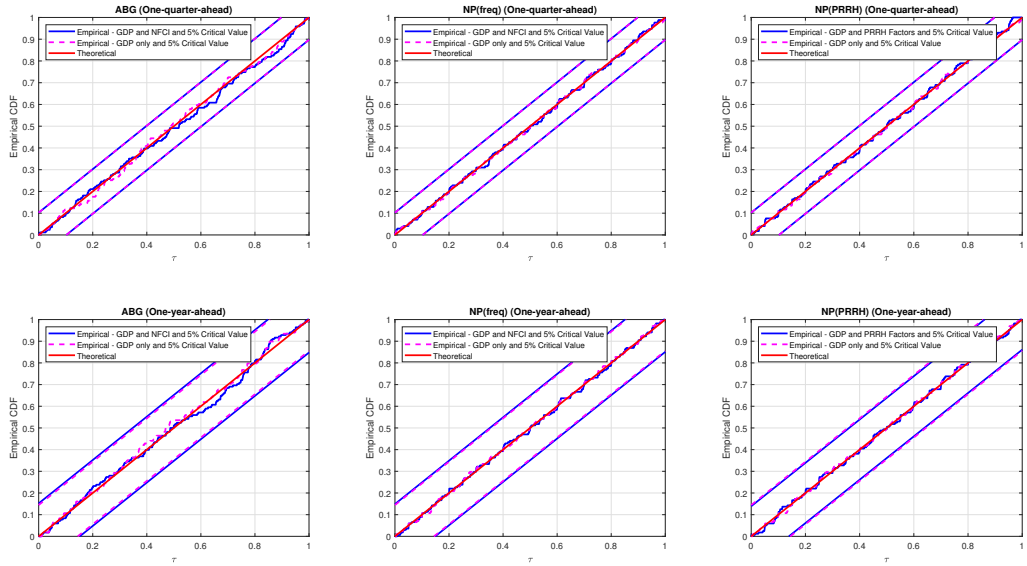

Notes: The figures show the empirical CDF of the PITs (blue line) from the QR models with the NFCI (and lagged GDP), the empirical CDF of the PITS (dashed red line) from the QR models without NFCI, the CDF of the PITs under the null hypothesis of correct calibration (the 45-degree line), and the 5% critical value bands of the Rossi and Sekhposyan (2019) PITs test.

Figure A32: CDF of the in-sample PITs (one-quarter-ahead forecasts, 1993Q1-2015Q4) and (one-year-ahead forecasts, 1993Q4-2015Q4) from ABG, NP(freq), and NP(PRRH)

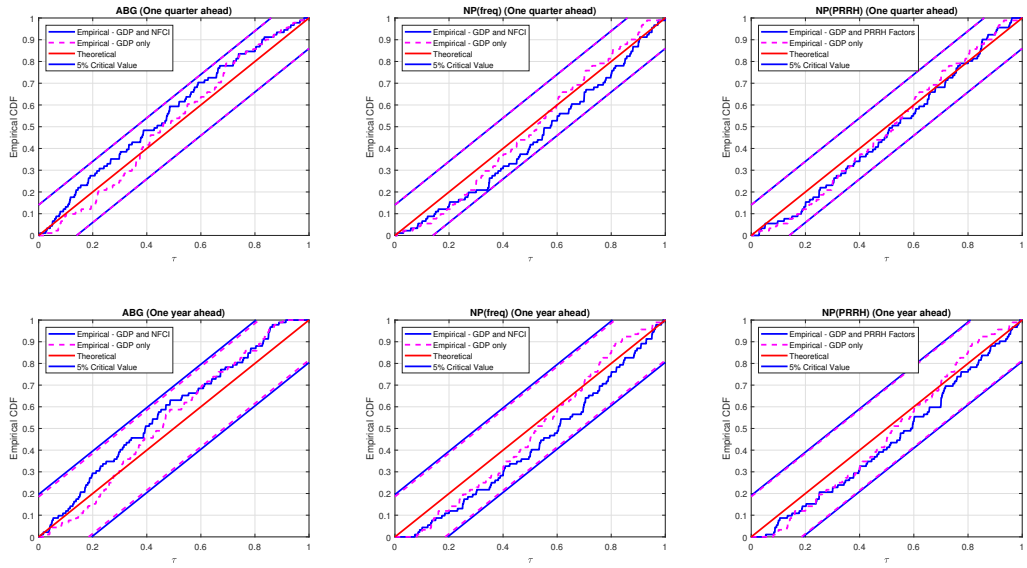

Notes: The figures show the empirical CDF of the PITs (blue line) from the QR models with the NFCI (and lagged GDP), the empirical CDF of the PITs (dashed red line) from the QR models without NFCI, the CDF of the PITs under the null hypothesis of correct calibration (the 45-degree line), and the 5% critical value bands of the Rossi and Sekhposyan (2019) PITs test.

Figure A33: CDF of the out-of-sample PITs from ABG, NP(freq), and NP(PRRH)

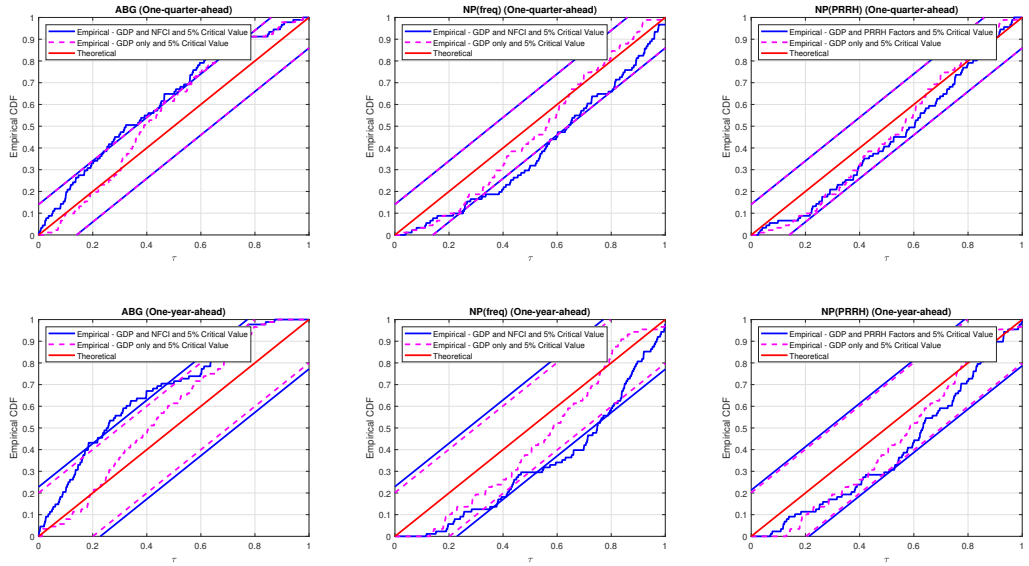

Notes: The figures show the empirical CDF of the PITs (red line), the CDF of the PITs under the null hypothesis of correct calibration (the 45-degree line) and the 5% critical value bands of the Rossi and Sekhposyan (2019) PITs test.